EPA

Measurement of Hydraulic Conductivity Distributions:

A Manual of Practice

EPA/600/8-90/046

MEASUREMENT OF HYDRAULIC CONDUCTIVITY DISTRIBUTIONS

A MANUAL OF PRACTICE

by

FRED J. MOLZ, OKTAY GÜVEN, JOEL G. MELVILLE
Civil Engineering Department
Auburn University, AL 36849

With Contributions By

ALFRED E. HESS and FREDERICK L. PAILLET
United States Geological Survey
Denver Federal Center
Denver, CO 80225

CR-813647

Project Officer

Lowell E. Leach
Robert S. Kerr Environmental Research Laboratory
Ada, OK 74820

ROBERT S. KERR ENVIRONMENTAL RESEARCH LABORATORY
OFFICE OF RESEARCH AND DEVELOPMENT
U.S. ENVIRONMENTAL PROTECTION AGENCY
ADA, OK 74820

DISCLAIMER

The information in this document has been funded wholly or in part by the United States Environmental Protection Agency under assistance agreement number CR-813647 to the Board of Trustees of Auburn University, Auburn, Alabama, subjected to the Agency's peer and administrative review, and it has been approved for publication as an EPA document. Mention of trade names or commercial products does not constitute endorsement or recommendation for use.

FOREWORD

EPA is charged by Congress to protect the Nation's land, air and water systems. Under a mandate of national environmental laws focused on air and water quality, solid waste management and the control of toxic substances, pesticides, noise and radiation, the Agency strives to formulate and implement actions which lead to a compatible balance between human activities and the ability of natural systems to support and nurture life.

The Robert S. Kerr Environmental Research Laboratory is the Agency's center of expertise for investigation of the soil and subsurface environment. Personnel at the laboratory are responsible for management of research programs to: (a) determine the fate, transport and transformation rates of pollutants in the soil, the unsaturated and saturated zones of the subsurface environment; (b) define the processes to be used in characterizing the soil and subsurface environment as a receptor of pollutants; (c) develop techniques for predicting the effect of pollutants on ground water, soil, and indigenous organisms; and (d) define and demonstrate the applicability and limitations of using natural processes, indigenous to the soil and subsurface environment, for the protection of this resource.

This manual of practice presents state-of-the-art techniques for field measurements of the vertical distribution of hydraulic conductivity in contaminated ground water aquifers for more accurate characterization of Superfund and other sites. These field techniques allow fully three-dimensional characterization of aquifer properties which can be used in advection-dominated transport models to significantly enhance our ability to understand and predict contaminant transport, reaction and degradation in the field. The techniques also provide data for optimum placement of well screens for remediation and monitoring.

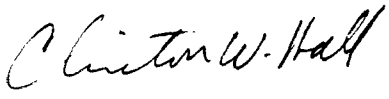

Clinton W. Hall
Director
Robert S. Kerr Environmental
Research Laboratory

ABSTRACT

The ability of hydrologists to perform field measurements of aquifer hydraulic properties must be enhanced in order to significantly improve the capacity to solve ground water contamination problems at Superfund and other sites. The primary purpose of this manual is to provide new methodologies for measuring K(z), the distribution of horizontal hydraulic conductivity in the vertical direction in the vicinity of a test well. Measurements in nearby wells can then be used to estimate three-dimensional distributions. As dispersion-dominated models (particularly two-dimensional, vertically-averaged models) approach their limitations, it is becoming increasingly important to develop two-dimensional vertical profile or fully three-dimensional advection-dominated transport models in order to significantly increase the ability to understand and predict contaminant transport, reaction, and degradation in the field. Such models require the measurement of hydraulic conductivity distributions, K(z), rather than vertically averaged values in the form of transmissivities.

Three devices for measuring K(z) distributions (the impeller flowmeter, the heat-pulse flowmeter, and a multi-level slug test apparatus) are described in detail, along with application and data reduction procedures. Results of the various methods are compared with each other and with the results of tracer studies. The flowmeter approach emerged as the best candidate for routine K(z) measurements. Impeller meters are now available commercially, and the more sensitive flowmeters (heat pulse and electromagnetic) are expected to be available in the near future.

CONTENTS

FIGURES

TABLES

LIST OF ABBREVIATIONS AND SYMBOLS

Abbreviations

Br	Bromide
CPM	counts per minute
EFLOW	computer code name
EPA	Environmental Protection Agency
IGWMC	International Ground Water Modeling Center
NWWA	National Water Well Association
OTA	Office of Technology Assessment
USGS	United States Geological Survey

Symbols

A	screen area per unit length, (L)
A_c	open cross-sectional area of casing, (L^2)
B	slope of semi-log plot, (T^{-1})
B,b	aquifer thickness, (L)
D	aquifer thickness, (L)
H	distance from confining layer to straddle packer, (L)
h	hydraulic head, (L)
h_o	initial head, (L)
i	counting index, (-)
K	hydraulic conductivity, (L/T)
K_r	hydraulic conductivity in radial direction, (L/T)
K_z	hydraulic conductivity in vertical direction, (L/T)
$\bar{K}$	vertically-averaged hydraulic conductivity, (L/T)
L	length, (L)
P	dimensionless flow parameter, (-)
Q	discharge rate, (L^3/T)
QP	pumping rate, (L^3/T)
q	Darcy velocity, (L/T)
r	radius, (L)
r_c	casing radius, (L)
R_e	radius of influence, (L)
r_p	plunger radius, (L)
r_w	well radius, (L)
S	storage coefficient, (-)
S_s	specific storage, (L^{-1})
T	transmissivity, (L^2/T)
t	time, (T)
U	Darcy velocity, (L/T)
V	pore or seepage velocity vector, (L/T)
V_r	radial seepage velocity, (L/T)
x,y	horizontal coordinates, (L)
y(t)	head change in slug test, (L)
y_o	initial head change, (L)
Z,z	vertical coordinates, (L)
α_r	radial dispersivity, (L^{-1})
α_v	vertical dispersivity, (L^{-1})

---

* Generalized symbols for the dimensions of length, time and mass will be L, T, and M respectively. The symbol (-) indicates a dimensionless quantity.

Δ	prefix symbol indicating "change in", (-)
∇	gradient operator, (-)
π	3.14159, (-)
Θ	porosity, (-)

EXECUTIVE SUMMARY

INTRODUCTION

In order to significantly improve the ability to understand ground-water contamination problems at Superfund and other sites, it has become necessary to improve the ability to make field measurements. The single most important parameter concerning contaminant migration is hydraulic conductivity. Conventionally, pumping tests with fully penetrating wells are used to determine transmissivity and longitudinal dispersion coefficients to describe contaminant spreading in the direction of flow. Models used for making these predictions are dispersion-dominated.

Horizontal hydraulic conductivities can be defined as a function of vertical position (K(z)). When this is done at a number of locations in the horizontal plane, the resulting data can serve as a basis for developing two-dimensional vertical cross-section, quasi three-dimensional or fully three-dimensional flow and transport models.

Shown in Figure I-9 are dimensionless K(z) distributions obtained at four different scales in a single well using an impeller meter. As the measurement interval varies from 10 ft (3.05 m) to 1 ft (0.305 m), the apparent variability of the hydraulic conductivity increases. This is the type of information that is lost when fully-penetrating pumping tests are used to obtain vertically-averaged hydraulic conductivities.

There are several techniques for making vertically-distributed measurements, including flowmeter and multilevel slug tests. These serve as the basis for an improved understanding of subsurface transport pathways which allow the application of new contaminant transport models that are advection-dominated and largely free of the problems associated with scale-dependent dispersion coefficients.

SELECTED METHODOLOGY

Two techniques for obtaining K(z) information will be discussed. These are the flowmeter and multi-level slug test methods. Of the two, the flowmeter method is more responsive, less sensitive to near-well disturbances due to drilling, and easier to apply. As illustrated in Figure I-2, a flowmeter test involves measuring the steady pumping rate, QP, and the flow rate distribution along the borehole or well screen, Q(z).

Various types of flowmeters have been devised for measuring Q(z). Those most sensitive to low flows are heat-pulse, electromagnetic, or tracer-release technology, but such instruments are not presently available commercially. Impeller meters (commonly called spinners) have been used for several decades in the petroleum industry, and a few suitable for ground-water applications are available.

IMPELLER METER TESTS

Impeller meter tests can be a relatively quick and convenient method for obtaining information about the vertical variation of horizontal hydraulic conductivity as illustrated in Figure I-2. A caliper log is first run to determine the screen diameter so that variations can be taken into account when calculating discharge. A small pump is operated at a constant flow rate, QP, until a pseudo steady-state is obtained. The flowmeter is lowered to near the bottom of the well, and a measurement of discharge is obtained by impeller generated electrical pulses over a selected period of time. The meter is then raised a few feet and another reading taken. This procedure continues until the water table is reached. The result is a series of data points giving vertical discharge, Q, within the well screen as a function of vertical position z. Just above the top of the screen the meter reading should be equal to QP, the steady pumping rate that is measured independently at the surface with a water flowmeter. The procedure may be repeated several times to ascertain that readings are stable.

HEAT-PULSE FLOWMETER TESTS

The use of the impeller meter is limited when the presence of low permeability materials preclude pumping at a rate sufficient to operate an impeller. The impeller operates with a minimum velocity from about 3 to 10 ft/min (1 to 3 m/min). The heat-pulse flowmeter can be used as an alternative to an impeller meter in virtually any application due to its greater sensitivity. It has a measurement range from 0.1 to 20 ft/min (0.03 to 6.1 m/min).

The basic principle of the heat-pulse flowmeter is to create a thin horizontal disc of heated water within the well screen at a known time and a known distance from two thermocouple heat sensors, one above and one below the heating element. As the heat moves with the upward or downward water flow, the time required for the temperature peak to arrive at one of the heat sensors is recorded. The apparent velocity is then given by the known travel distance divided by the recorded travel time. Thermal buoyancy effects are eliminated by raising the water temperature by only a small fraction of a centigrade degree. The geometry associated with the heat-pulse flowmeter is shown in Figure III-2.

Hopefully, thermal flowmeters now being developed by the U.S. Geological Survey, and other sensitive devices, such as the electromagnetic flowmeter being developed by the Tennessee Valley Authority, will be available commercially in the near future.

MULTILEVEL SLUG TESTS

The flowmeter testing procedure is generally superior to the multilevel slug test approach, because the latter depends on the ability to hydraulically isolate a portion of the test aquifer using a straddle packer. However, if reasonable isolation can be achieved, the multilevel slug test is a viable procedure for measuring K(z). All equipment needed for such testing is available commercially, and there is an additional advantage of not requiring an injection or withdrawal of water from the test well.

The testing apparatus used in a multilevel slug test is illustrated in Figure II-1. Two inflatable packers separated by a length of perforated pipe comprise the straddle packer assembly. A larger packer, referred to as the reservoir packer, is attached to the straddle packer creating a unit of fixed length which can be moved to desired positions in the well. When inflated, the straddle packer isolates the desired test region of the aquifer and the reservoir packer isolates a reservoir in the casing above the multilevel slug test unit and below the potentiometric surface of the confined aquifer.

In a typical test, water is displaced in the reservoir above the packer creating a head which induces flow through the central core of the reservoir packer to the straddle packer assembly. Water then flows from the perforated pipe, through the slotted well screen, into the test region of the aquifer.

Typical results of a series of tests at different elevations are shown in Figure II-3. The data result from a plunger insertion causing a sudden reservoir depth increase to approximately y_o=3 ft. The depth variation, y=y(t), is a result of flow into the aquifer test section adjacent to the straddle packer. The different slopes of the straight line approximations reflect the variability of the hydraulic conductivity in the aquifer at the different test section elevations. From this data hydraulic conductivity distributions can be calculated.

CHAPTER I

THE IMPELLER METER METHOD FOR MEASURING HYDRAULIC CONDUCTIVITY DISTRIBUTIONS

I-1 INTRODUCTION

One of the better existing methodologies for obtaining vertically distributed hydraulic conductivity information is the borehole impeller meter test. It may be viewed as a generalization of a fully penetrating pumping test except that in addition to measuring the steady pumping rate, QP, the flow rate distribution along the borehole or well screen, Q(z), is recorded as well.

Various types of flowmeters have been devised for measuring Q(z), and described in the literature (Hada, 1977; Keys and Sullivan, 1978; Schimschal, 1981; Hufschmied, 1983; Hess, 1986; Morin et al., 1988a; Rehfeldt et al., 1988; Molz et al., 1989a,b). Most low-flow-sensitive types of meters are based on heat-pulse, electromagnetic or tracer-release technology (Keys and MacCary, 1971; Hess, 1986), but such instruments are not presently available commercially, although several are nearing this stage of development. Impeller meters (commonly called spinners) have been used for several decades in the petroleum industry and a few are suitable for ground-water applications. Hufschmied (1983) and Rehfeldt et al. (1988) have reported such investigations, the latter being the most detailed to date regarding the assumptions made in using a borehole impeller meter to measure hydraulic conductivity as a function of vertical position.

The purpose of this chapter is to describe the application of an impeller meter to measure K(z) at various locations in the horizontal plane. The site used for this work is illustrated in Figure I-1 and, as shown, consists of interbedded sands and clays with the water table being about 3 m (9.84 ft) below the land surface.

I-2 PERFORMANCE AND ANALYSIS OF IMPELLER METER TESTS

I-2.1 Background Information

Impeller meter tests, illustrated in Figure I-2, can be a relatively quick and convenient method for obtaining information about the vertical variation of horizontal hydraulic conductivity. A caliper log is first run to determine the screen diameter so that variations can be taken into account when calculating discharge. A small pump is operated at a constant flow rate, QP, until a pseudo steady state is obtained. The flowmeter is lowered to near the bottom of the well, and a measurement of discharge is obtained by counting impeller generated electrical pulses over a selected period of time. The meter is then raised a few feet and another reading taken. This procedure continues until the top of the water table is reached. The result is a series of data points giving vertical discharge, Q, within the well screen as a function of vertical position z. Just above the top of the screen the meter reading should be equal to QP, the steady pumping rate that is measured independently at the surface with a water flowmeter. The procedure may be repeated several times to ascertain that readings are stable.

While Figure I-2 applies explicitly to a confined aquifer, application to an unconfined aquifer is similar. Most impeller meters are capable of measuring upward or downward flow, so if the selected pumping rate, QP, causes excessive drawdown, one can employ an injection procedure as an alternative. In either case, there will be unavoidable errors near the water table due to the deviation from horizontal flow. It is desirable in unconfined aquifers to keep QP as small as possible, consistent with the stall velocity of the meter. Thus, more sensitive meters will have an advantage for unconfined aquifers.

As shown in Figure I-3, data analysis assumes that the aquifer is composed of a series of n horizontal layers. The difference between two successive meter readings yields the net flow, ΔQ_i, entering the screen

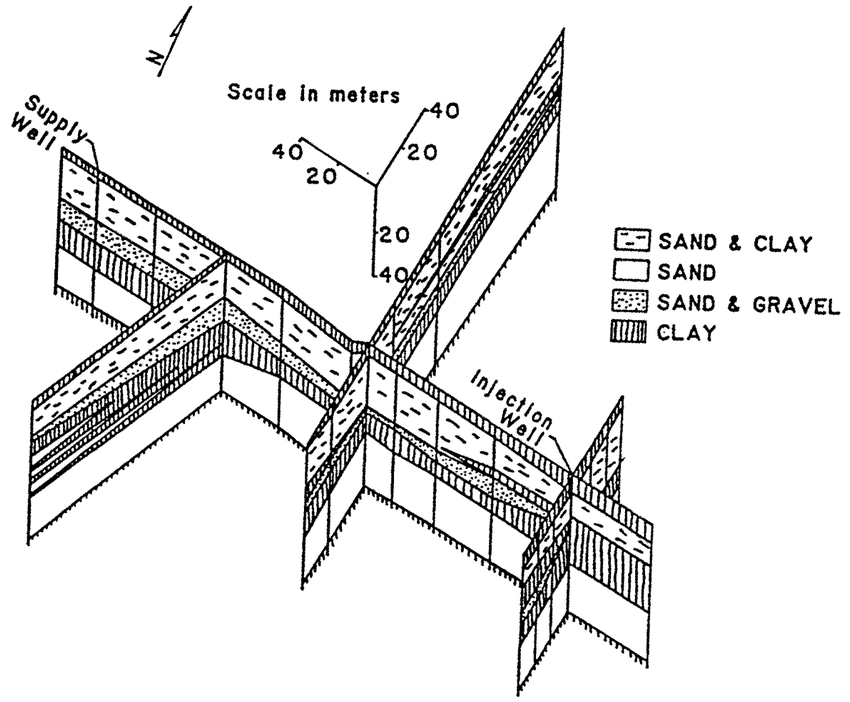

Figure I-1. Subsurface Hydrologic System.

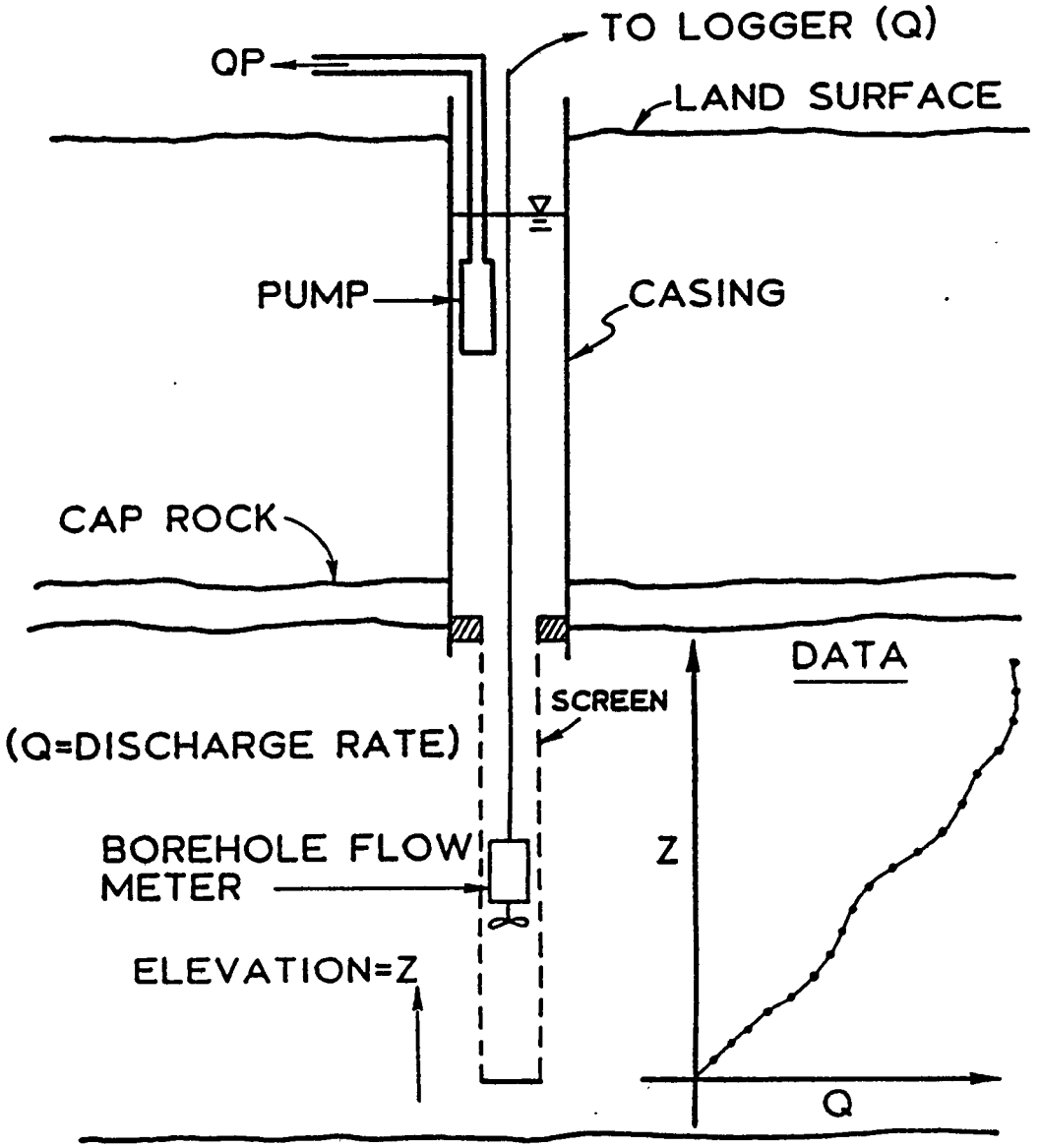

Figure I-2. Apparatus and Geometry Associated with a Borehole Flowmeter Test.

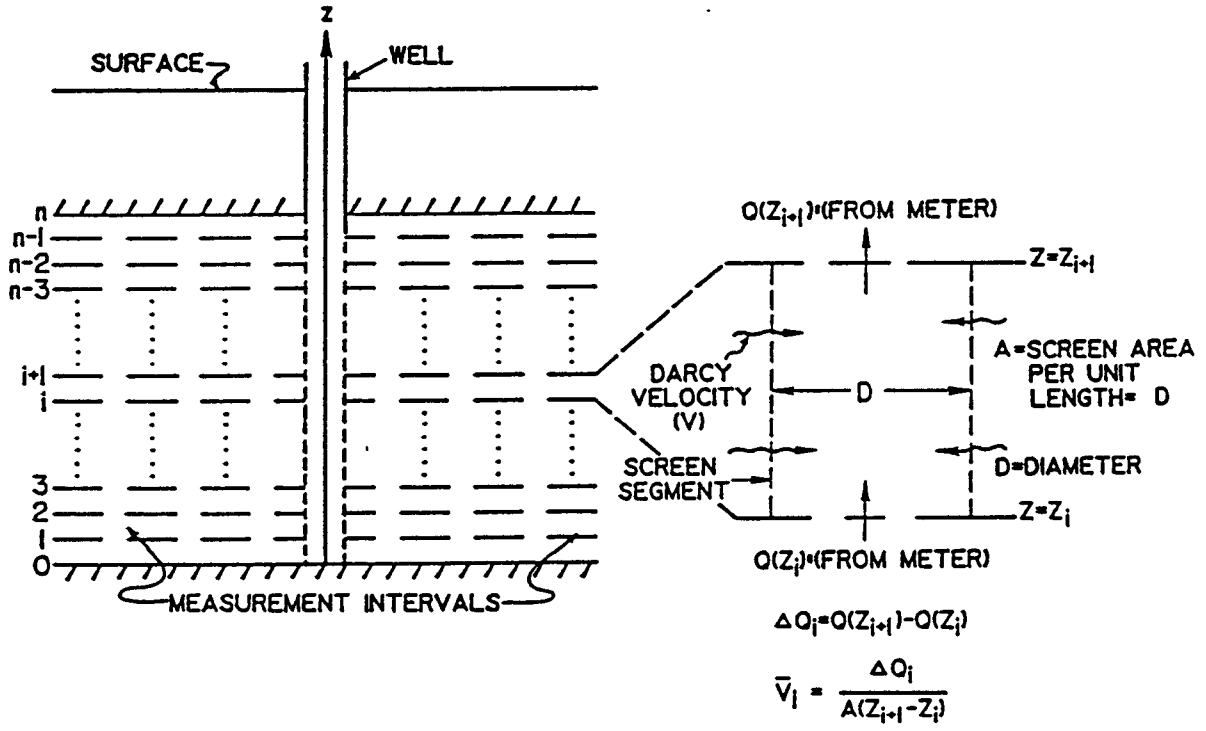

Figure I-3. Assumed Layered Geometry within which Impeller Meter Data are Collected and Analyzed. Q(z) is Discharge Measured at Elevation z.

segment between the elevations where the readings were taken. The Cooper-Jacob [1946] formula for horizontal flow to a well from a layer, i, of thickness Δz_i, given by:

$$\Delta H_i(r_w,t) = \frac{\Delta Q_i}{2\pi K_i \Delta z_i} \ln\left[\frac{1.5}{r_w}\frac{K_i(\Delta z_i)t}{S_i}\right] \qquad \text{(I-1)}$$

where ΔH_i = drawdown in ith layer, ΔQ_i = flow from ith layer into the well, K_i = horizontal hydraulic conductivity of the ith layer, Δz_i = ith layer thickness, r_w = effective well radius, t = time since pumping started, and S_i = storage coefficient for the ith layer. Solving equation (I-1) for the K_i outside of the log term yields:

$$K_i = \frac{\Delta Q_i}{2\pi \Delta H_i \Delta z_i} \ln\left[\frac{1.5}{r_w}\frac{K_i(\Delta z_i)t}{S_i}\right] \qquad \text{(I-2)}$$

which can be solved iteratively to obtain a value for K_i. Further details may be found in Morin et al. [1988a] or Rehfeldt et al. [1988].

A convenient alternative method for obtaining a K distribution is based on the study of flow in a stratified aquifer by Javandel and Witherspoon [1969] which showed that in idealized, layered aquifers, flow at the well bore radius, r_w, rapidly becomes horizontal even with relatively large permeability contrasts between layers. Under such conditions, radial gradients along the well bore are constant and uniform, and flow into the well from a given layer is proportional to the transmissivity of that layer, that is:

$$\Delta Q_i = \alpha \Delta z_i K_i \qquad \text{(I-3)}$$

where α is a constant of proportionality. This condition occurs when the dimensionless time $t_D = \bar{K}t/S_s r_w^2$ is $\geq$ 100. In this expression $\bar{K}$ is the average horizontal aquifer hydraulic conductivity defined as $\Sigma K_i \Delta z_i/b$, where b is aquifer thickness, S_s is the aquifer specific storage, t is time since pumping started and r_w is well bore radius.

To solve for α, sum the ΔQ_i over the aquifer thickness, to get:

$$\sum_{i=1}^{n} \Delta Q_i = QP = \alpha \sum_{i=1}^{n} \Delta z_i K_i \qquad \text{(I-4)}$$

Multiplying the right-hand side of equation (I-3) by b/b and solving for α yields:

$$\alpha = \frac{QP}{b\bar{K}} \qquad \text{(I-5)}$$

Finally, substituting for α in equation (I-3) and solving for $K/\bar{K}$ gives:

$$\frac{K_i}{\bar{K}} = \frac{\Delta Q_i/\Delta z_i}{QP/b}; \; i = 1, 2, \ldots n \qquad \text{(I-6)}$$

To obtain equation (I-6) it was assumed that steady state conditions apply and therefore ΔQ_i and QP do not change with time. This will occur when $r_w^2 S/4Tt < 0.01$, where S and T are aquifer storage coefficient and transmissivity, respectively. Thus, from the basic data a plot of K/K can be obtained if a value of $\bar{K}$ from a fully penetrating pumping test is available. The K/K approach has practical appeal because one does not have to know values for r_w or S_i, which are impossible to specify precisely. Also, multiplicative errors in flowmeter readings are cancelled out, and the meter does not have to be calibrated. However, a fully penetrating pumping test or slug test must be performed along with each flowmeter test.

While the data analysis involved in a flowmeter test is simple, care must be taken to satisfy all assumptions so that only the flow caused by pumping is measured (Rehfeldt et al., 1988). For example, an existing ambient flow must be measured prior to pumping so that initial flow conditions are known. Alternatively, a two-step pumping procedure can be used (Rehfeldt et al., 1988). In addition, data analysis procedures assume horizontal flow and that head loss is due only to water flow through the undisturbed formation. There are screen and head losses within the well; however, these can be minimized by pumping at the lowest rate consistent with the stall velocity of the impeller meter. For a much more detailed discussion of well head losses and their possible correction see Rehfeldt et al. (1988). Local deviations from horizontal flow will exist in most aquifers, but the effects should be of second order compared to those of the average flow field as long as the measurement intervals are not too small. As Δz_i gets smaller, errors due to deviations from horizontal flow become larger which leads to poor repeatability of flowmeter readings obtained from multiple tests performed in the same well.

I-2.2 Example Application

Data used in this example were obtained from tests at a site north of Mobile, Alabama, which is illustrated in Figure I-1. Testing began with a mild redevelopment and cleaning of the test well screens (Fig. I-4) with air followed by ambient flow measurements using a heat-pulse flow meter developed by the U.S. Geological Survey which has a measurement range of 0.1 to 20 ft/min (0.03 to 6.1 m/min.) (Hess, 1986). This is about 10 times more sensitive than any impeller meter. Even at this sensitivity no ambient vertical flow within the screen could be detected, which is consistent with the assumption that the aquifer is relatively permeable, well confined, and the horizontal gradient is low. If a significant ambient vertical flow had existed at any level Δz_i, it would have been subtracted from the impeller meter reading for that level prior to data analysis.

The test well is illustrated in Figure I-2. It has a 4 in (10 cm) ID well screen (0.01 inch slotted plastic or plastic wire-wrap, see Fig. I-4) extending from about 130 ft (39.6 m) to 200 ft (61 m) below the land surface. None of the screens are sand packed. The well screens were cleaned with air, and caliper and ambient pressure logs were run. Caliper log data were used to verify and compute the cross-sectional area of the well, and the pressure log served to establish a hydraulic-head distribution for use as a reference in evaluating ΔH_i produced by pumping. A pressure transducer and an impeller meter with centralizer were lowered into the well, followed by a small submersible pump capable of pumping about 60 gpm (227 liter/min). After starting, the pump was allowed to run for about an hour, prior to taking pressure and impeller meter readings, to obtain pseudo-steady-state conditions as defined by the Cooper-Jacob criterion discussed previously. Data analysis showed that ΔH_i varied only slightly over the length of the screens.

An impeller meter can function in either a stationary or a trolling mode. In the stationary mode the meter is held at a series of set elevations, and readings are taken in the form of pulses per unit time with the aid of an electronic pulse counter. In the trolling mode, the meter is raised or lowered at a constant rate, and the reading reflects a superposition of the trolling and water flow velocities. For fine-scale ground-water applications, the stationary mode seems better suited; however, both methods of data acquisition were used during this study. Listed in Table I-1 are the basic impeller meter data obtained in wells E7, and A5, along with the corresponding head difference between static and pumping conditions derived from the pressure logs. In order to convert impeller meter readings into discharge, the meter was calibrated by placing it in the unslotted top extension of each well screen and pumping at three different rates which were measured independently at the surface. In all cases the response was found to be linear. For wells E7 and A5, the calibration equation was $Q = 0.00428(CPM)$, where Q is in ft^3/min and CPM represents impeller "counts per minute." Applying this equation to the data listed in Table I-1 resulted in the discharge profiles presented in Table I-2.

I-2.3 Data Analysis

As discussed earlier, there are two procedures for inferring a hydraulic conductivity function, K(z), from impeller meter data. One approach involves the application of equation (I-2) to each depth interval. This was done for data obtained at wells A5 and E7 using a storage coefficient, $S_i = 10^{-5}\ \Delta z_i$, and an average specific storage of $10^{-5}ft^{-1}$ ($3.05 \times 10^{-6}m^{-1}$) determined from a previously performed pumping test (Parr et al., 1983). The results are presented in Table I-3 as K1(z), with depth values corresponding to the midpoint of the assumed layers. Also shown in Table I-3, as K2(z), are the results of applying equation (I-6) to each measurement interval. To obtain these results, values of the dimensionless function $K_i/\bar{K}$ were calculated, where $\bar{K}$ is the average hydraulic conductivity obtained from a standard, fully penetrating pumping test in the vicinity of E7 and

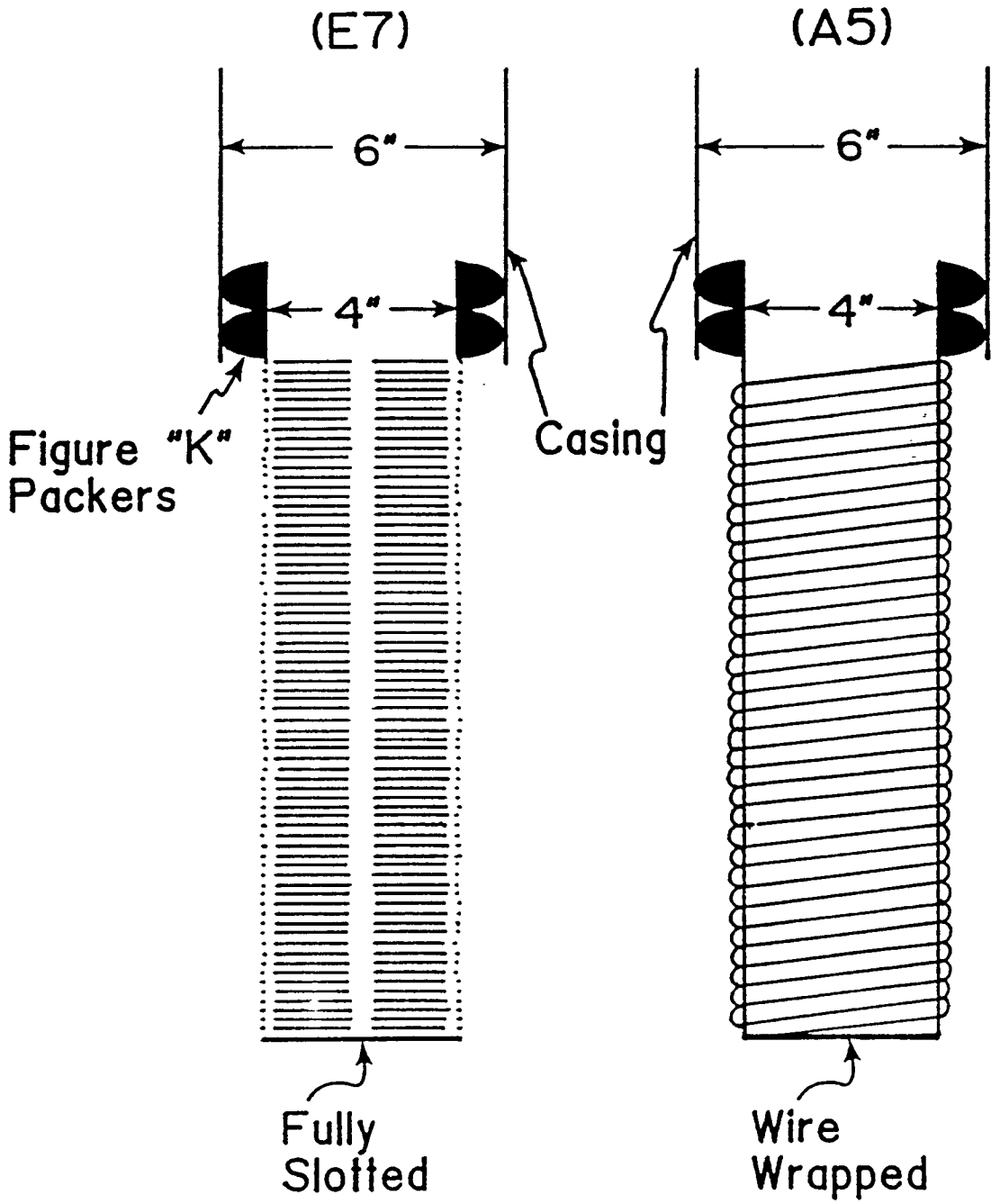

Figure I-4 Details of Screen Types in Wells E7 and A5.

TABLE I-1. IMPELLER METER (DISCRETE MODE) AND DIFFERENTIAL HEAD DATA OBTAINED IN WELLS E7 AND A5 AT THE MOBILE SITE.
(z=depth, CPM=counts per minute, and ΔH=head difference between static and dynamic conditions)

Well #E7			Well #A5		
z(ft)	CPM	ΔH(ft)	z(ft)	CPM	ΔH(ft)
130	1983	1.218	132.5	2024	1.210
135	1933	1.202	137.5	1968	1.201
140	1886	1.189	142.5	1885	1.170
145	1764	1.177	147.5	1799	1.147
150	1705	1.166	152.5	1652	1.136
155	1607	1.157	157.5	1488	1.132
160	1561	1.149	162.5	1362	1.132
165	1468	1.143	167.5	1106	1.132
170	1118	1.139	172.5	882	1.138
175	994	1.138	177.5	740	1.156
180	911	1.138	182.5	506	1.173
185	638	1.138	187.5	293	1.186
190	277	1.138	190.0	57	1.193

TABLE I-2. WELL SCREEN DISCHARGE AS A FUNCTION OF VERTICAL POSITION IN WELLS E7 and A5 AT THE MOBILE SITE.
(z=depth, Q=discharge rate in well screen)

Well #E7		Well #A5	
z(ft)	Q(ft^3/min)	z(ft)	Q(ft^3/min)
130	8.49	132.5	8.66
135	8.27	137.5	8.42
140	8.07	142.5	8.07
145	7.55	147.5	7.70
150	7.30	152.5	7.07
155	6.88	157.5	6.37
160	6.68	162.5	5.83
165	6.28	167.5	4.73
170	4.79	172.5	3.77
175	4.25	177.5	3.17
180	3.90	182.5	2.17
185	2.73	187.5	1.25
190	1.19	190.0	0.24

TABLE I-3. HYDRAULIC CONDUCTIVITY DISTRIBUTIONS INFERRED FROM INFERRED FROM IMPELLER METER DATA USING TWO DIFFERENT APPROACHES DESCRIBED HEREIN. (Depth z is in ft. and K(z) is in ft./min.)

Well #E7			Well #A5		
z	K1(z)	K2(z)	z	K1(z)	K2(z)
132.5	0.050	0.042	135	0.055	0.043
137.5	0.046	0.038	140	0.083	0.063
142.5	0.128	0.100	145	0.091	0.069
147.5	0.059	0.049	150	0.163	0.119
152.5	0.104	0.083	155	0.184	0.134
157.5	0.048	0.040	160	0.140	0.104
162.5	0.100	0.080	165	0.297	0.212
167.5	0.405	0.299	170	0.257	0.185
172.5	0.139	0.109	175	0.156	0.115
177.5	0.088	0.071	180	0.263	0.189
182.5	0.315	0.236	185	0.237	0.171
187.5	0.421	0.310	189	0.536	0.371
195.0	0.154	0.120	195	0.027	0.022

A5. Using a $\overline{K}$ of 0.121 ft/min (3.69 x 10^{-2}m/min), the corresponding values of K2(z) are listed in Table I-3 and the hydraulic conductivity profiles are plotted in Figure I-5.

I-2.4 Comparison of Impeller Meter Tests With Tracer Tests

An examination of Figure I-5 shows that the trends in the data are virtually identical for wells A5 and E7. There is also a fairly good agreement with the absolute (dimensional) values calculated for the hydraulic conductivity.

It is of interest to compare the hydraulic conductivity distributions inferred from the impeller meter data with those obtained previously using single well tracer tests (Molz et al., 1988). These tests involved one fully penetrating tracer injection well and one multilevel observation well located about 20 ft (6.1 m) away. A bromide tracer was injected at a constant rate through the injection well while water samples were collected periodically from up to 14 different elevations in the observation well. Bromide concentrations allowed the determination of travel times between the injection and observation wells as a function of elevation. From this information it is possible to infer a relative hydraulic conductivity distribution (Molz et al., 1988). There is no reason to expect a detailed agreement between the impeller meter results and the single-well tracer test results because the latter data reflect an average hydraulic conductivity value inferred over a travel distance of approximately 20 ft (6.1 m) and the impeller meter data are averaged over 360°. However, as shown in Figure I-6, the agreement is reasonably good, indicating that the overall trend in K(z) persists over the 20 ft (6.1 m) travel distance of the tracer test (Molz et al., 1988).

I-3 MEASUREMENT OF HYDRAULIC CONDUCTIVITY AT DIFFERENT SCALES USING IMPELLER METER TESTS AND PUMPING TESTS

The main purpose of this section is to describe the application of impeller meter tests and pumping tests so that the reader will develop an appreciation for the type and extent of hydraulic information that can be assembled at a particular site. Once again, the site chosen for this detailed application was the Mobile site. Vertical scale information was obtained using the impeller meter while fully penetrating pumping tests were employed for obtaining information at various lateral scales. The testing procedures where those described in previous sections. The fully penetrating pumping tests were analyzed using the Cooper-Jacob Method (Freeze and Cherry, 1979, or most any contemporary ground-water text).

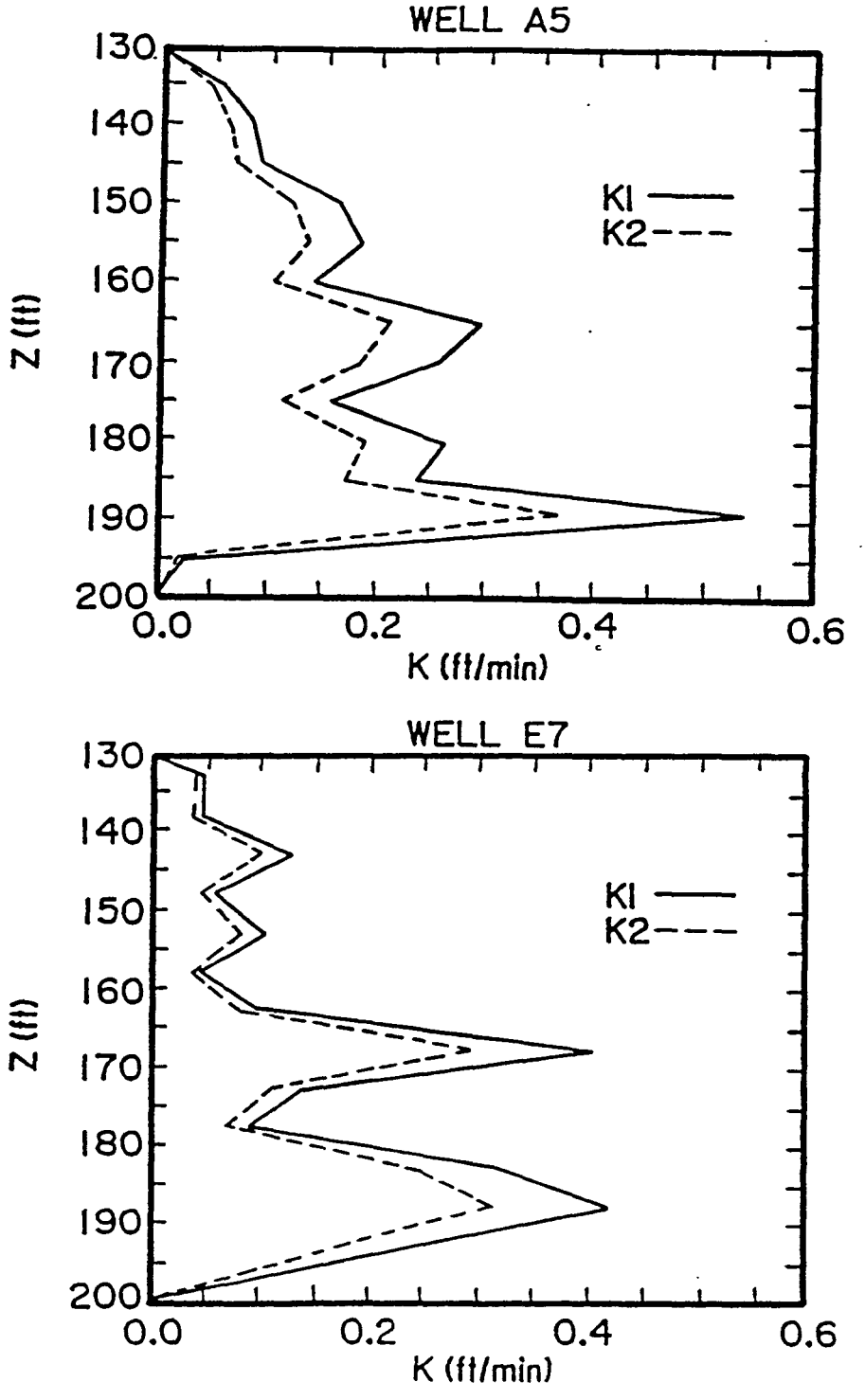

Figure I-5. Hydraulic Conductivity Distributions Calculated from Flowmeter Data Using Two Different Methods.

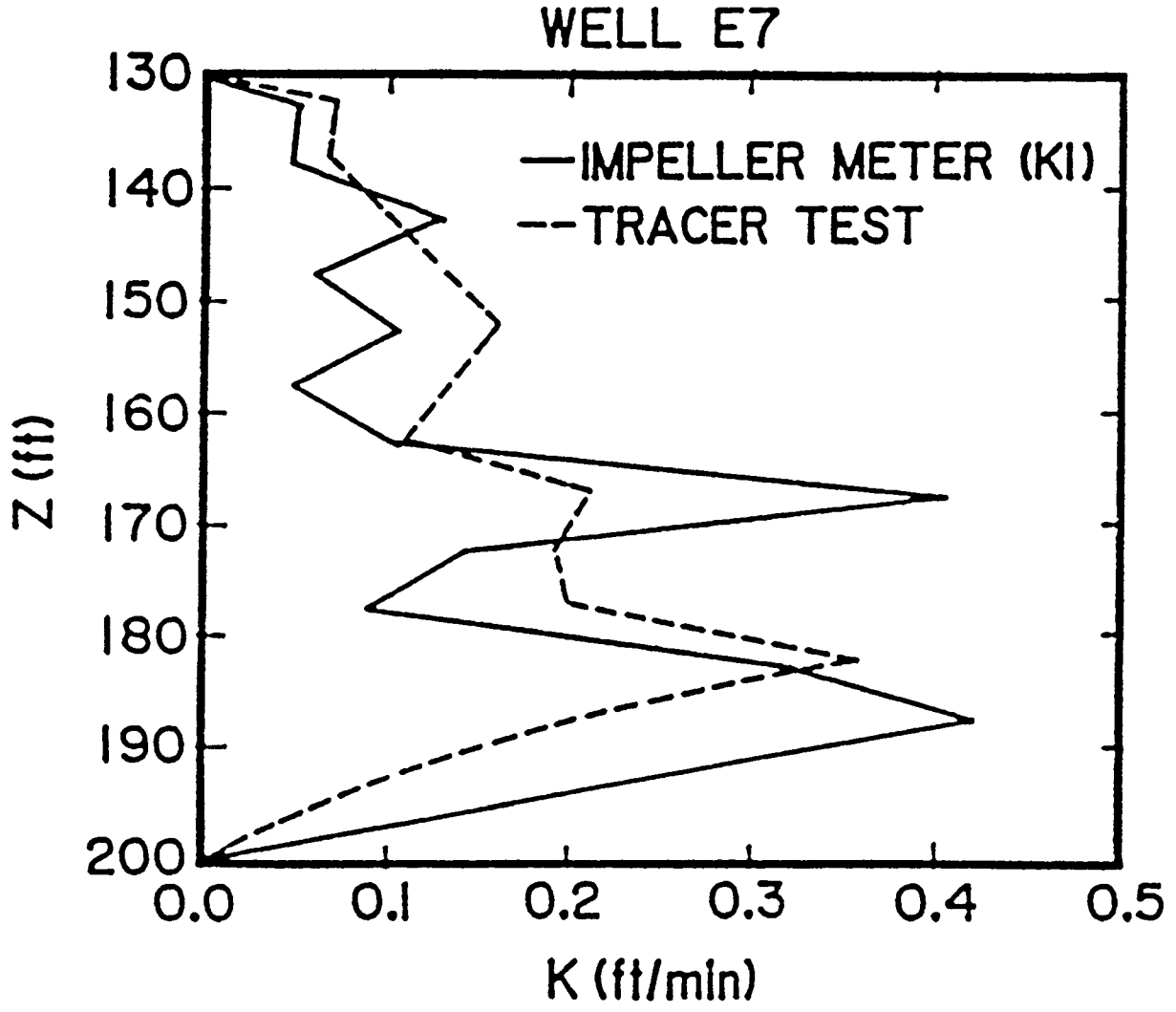

Figure I-6. Comparison of Hydraulic Conductivity Distributions for Well E7 Based on Tracer Impeller Meter Data.

I-3.1 Results of Tests

Shown in Figure I-7 is a plan view of the Mobile study site where the tests were performed. The various wells are designated as I2, E6, A3, etc. The number in parentheses next to each well is the vertically-averaged hydraulic conductivity in meters per day, K(x,y), that resulted from one or more small-scale pumping tests. Arrows indicate the pattern of testing, pointing from the observation well towards the pumping well. Each arrow represents a single test with a pumping rate of about 0.22 m^3/min (58 gpm). The repeatability of any one test was good with the drawdown data falling within 5% of each other.

A series of small-scale pumping tests were also performed in which the pumped wells were used as observation wells. Once again the pumping rate was approximately 0.22 m^3/min (58 gpm). The results of these tests are shown in Figure I-8.

A $K/\overline{K}$ distribution based on impeller meter tests performed in well E8 is shown in Figure I-9. The figure was obtained with the use of equation I-6 applied to impeller meter data from measurement intervals of 0.3 m (1 ft), 0.91 m (3 ft), 1.52 m (5 ft), and 3.108 m (10 ft).

As with the fully penetrating pumping tests, repeatability of the impeller meter tests was good. Evidence for this is shown in Figure I-10 which documents the results of repeated impeller meter tests in well E7.

I-3.2 Discussion of Results

The vertically-averaged hydraulic conductivity, $\overline{K}(x,y)$, shown in Figure I-7 seems to imply that the study aquifer is fairly homogeneous. The mean value of hydraulic conductivity is 54.9m/day with a standard deviation of only 2.4 m/day; however, since the data are correlated, the standard deviation is not well defined in a statistical sense and is used here only as a convenient measure of variation. The mean value agrees well with the result of a large-scale pumping test (53.4 m/day) performed previously using I2 as the pumping well and pumping at the rate of 1.48 m^3/min (390 gpm) (Parr et al., 1983).

As one would expect, the results shown in Figure I-8 are more variable because a pumping test using the pumping well as an observation well will sample a smaller volume of the aquifer. Here the mean value is only 3.5% smaller at 53.0 m/day, but the standard deviation has increased to 11.4 m/day.

No distinct pattern appears to emerge from Figure I-7 or Figure I-8. It is probable that $\overline{K}(x,y)$ will show lateral trends over distances in excess of 38 m, which is the approximate distance between wells I2 and E10, however, the variations here appear to be random.

Given the generally layered nature of geologic deposits in a fluvial environment, one would expect much more variability of horizontal hydraulic conductivity as a function of vertical position, K(z), than of vertically-averaged horizontal hydraulic conductivity as a function of lateral position, $\overline{K}(x,y)$. Examination of Figure I-9 shows this to be the case. Note that K(z) at any particular z is still averaged over the 360° polar angle, so that the impeller meter test gives no information about lateral heterogeneity or anisotropy around a given well.

Different degrees of heterogeneity are apparent at the various measurement scales of Figure I-9. As the measurement scale varies from 10 ft (3.05 m) to 1 ft (0.3 m), the measured variation in hydraulic conductivity increases, and there is every reason to expect that it would increase further if the measurement scale were decreased. Obviously, this type of heterogeneity is not reflected in the results of fully penetrating pumping tests.

I-4 SUMMARY AND CONCLUSIONS CONCERNING IMPELLER METER APPLICATIONS

Once the necessary equipment is obtained, impeller meter tests can be a relatively quick and convenient method for obtaining information about the vertical variation of horizontal hydraulic conductivity K(z) in an aquifer. This information can be used in a variety of ways including the design of monitoring wells or pump and treat systems. It can also be used as the basis for the development of three-dimensional flow and transport models which will be far more realistic than their vertically-averaged forerunners. (Applications to fractured rock hydrology are described in Chapter III.)

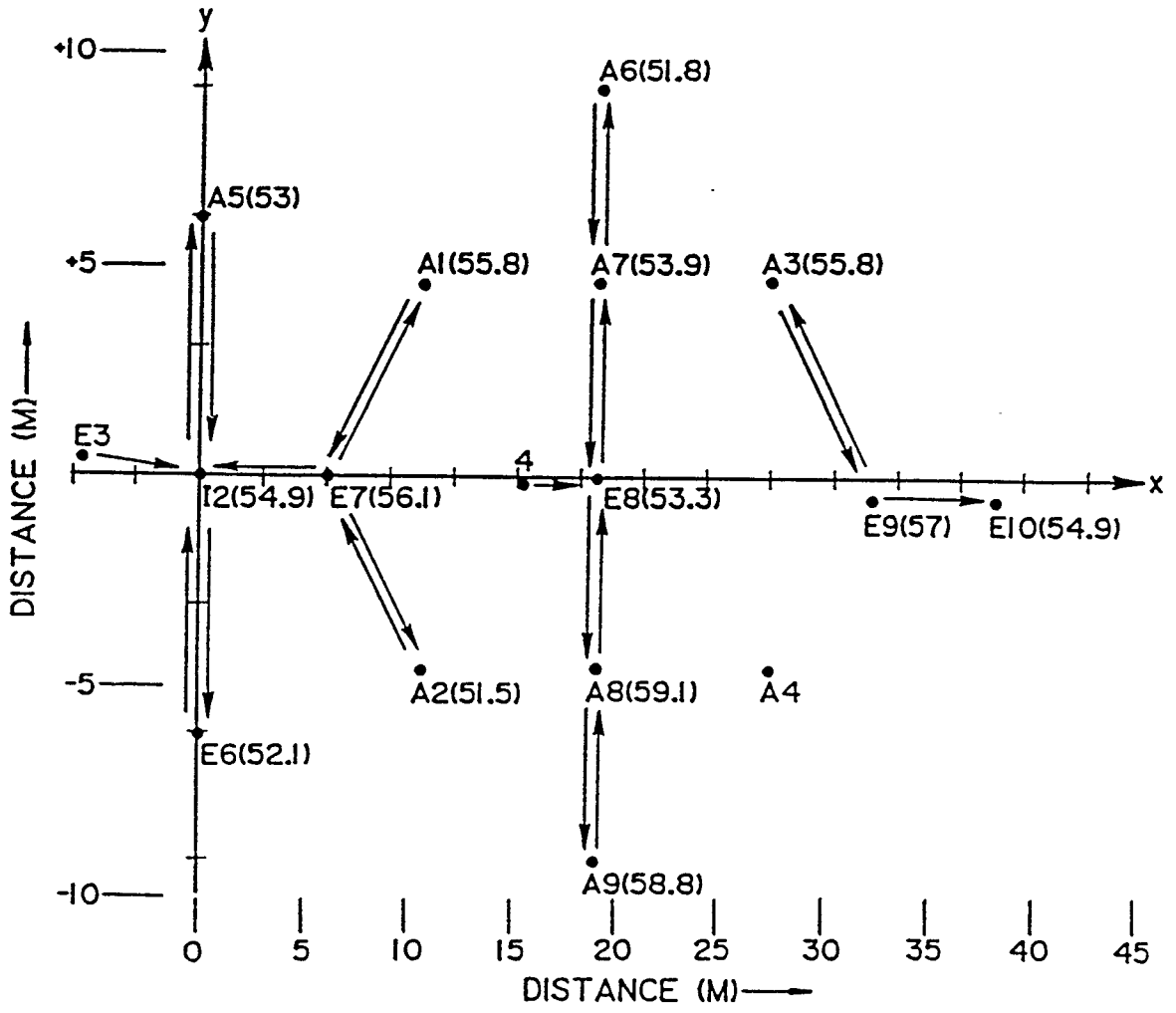

Figure I-7. Plan View of the Field Site where Small-Scale Pumping Tests were Performed.

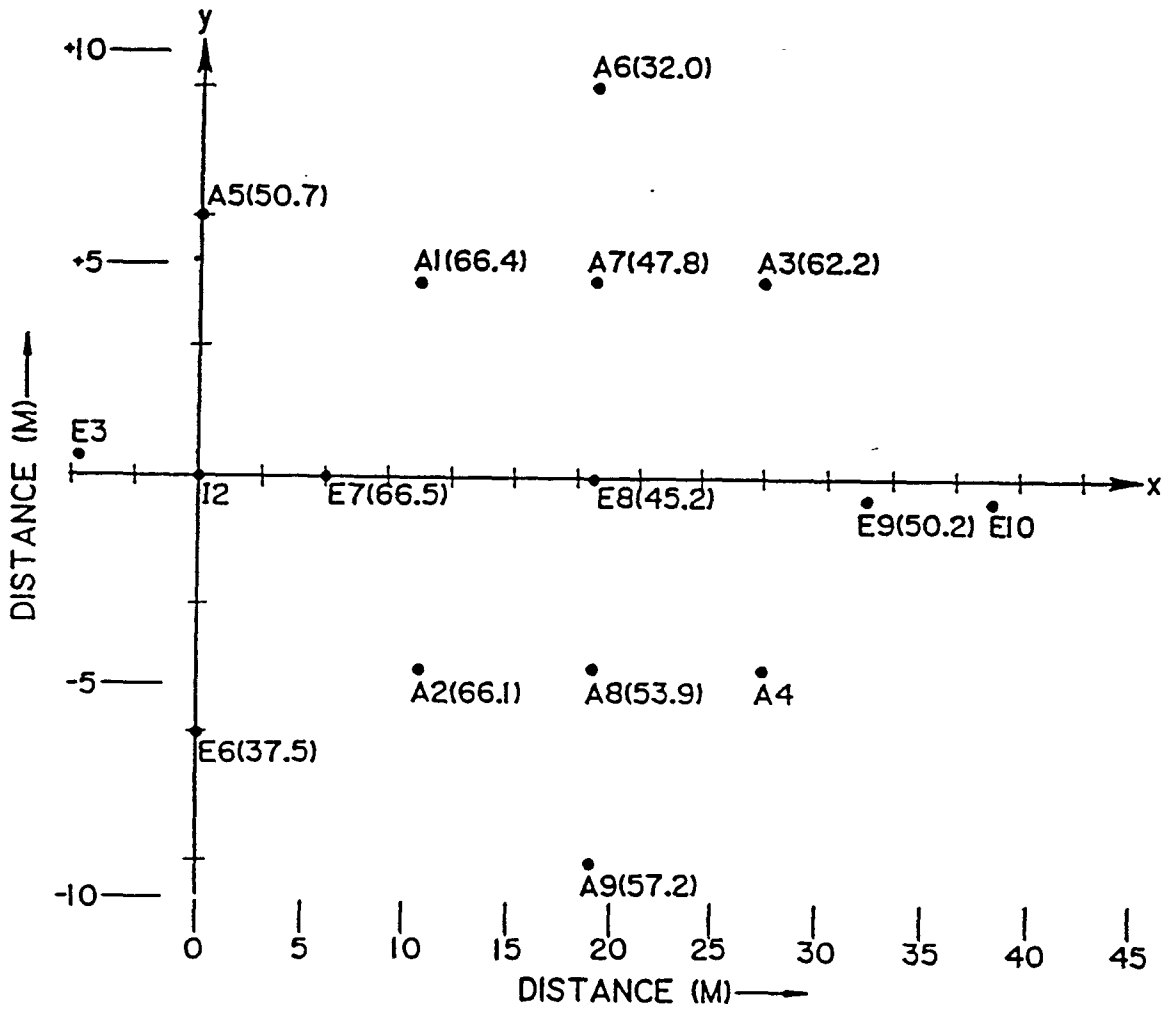

Figure I-8. Results of Small Scale Pumping Tests where Pumping Wells Were Used as Observation Wells.

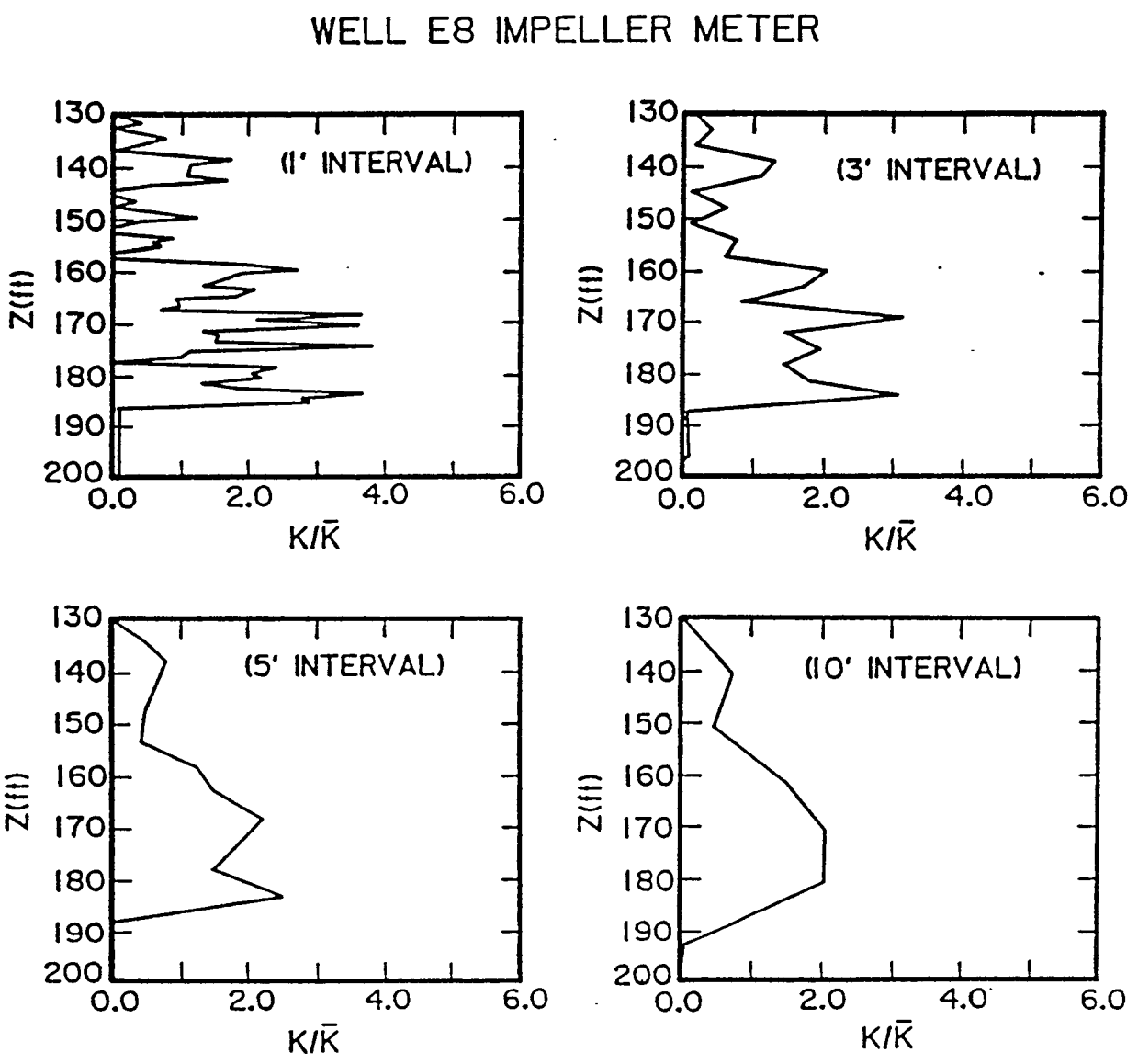

Figure I-9. Dimensionless Horizontal Hydraulic Conductivity Distributions Based On Impeller Meter Readings Taken at the Various Measurement Intervals Indicated on the Figure.

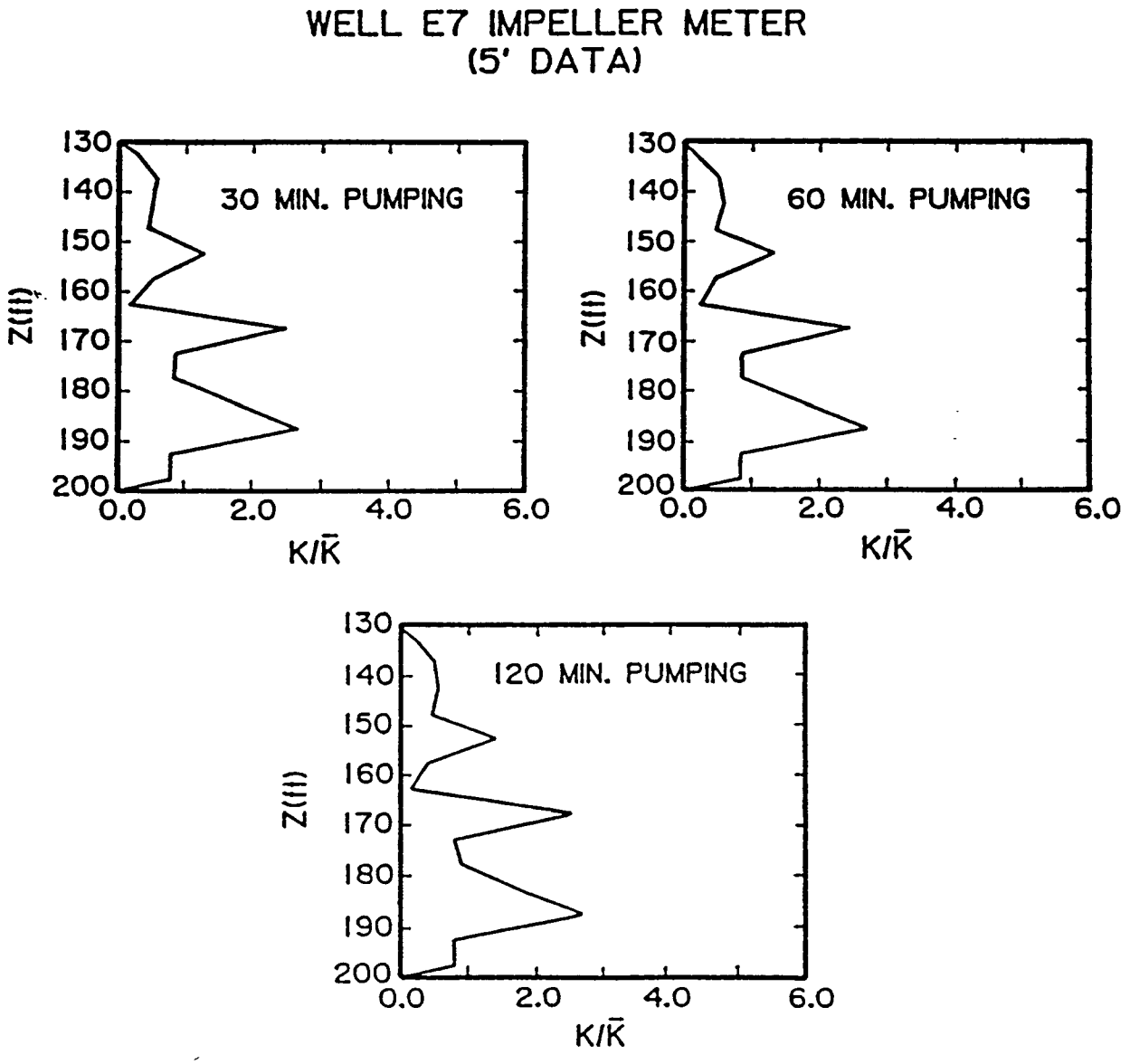

Figure I-10. Dimensionless Hydraulic Conductivity Distributions at Five Foot Intervals in Well E7 Taken 30 min., 60 min., and 120 min. after the Start of Pumping. The Results Show Good Repeatability of the Impeller Meter Method.

Over the past several years at the Mobile site, a fairly large amount of hydraulic conductivity data have been developed based in part on fully penetrating pumping tests, both large and small scale, and impeller meter tests. As far as contaminant transport predictions are concerned, the pumping tests alone are of limited use because, by their nature, they fail to show the large amount of vertically-distributed heterogeneity that is apparent to varying degrees in the impeller meter tests. Although obvious, this fact merits emphasis because fully penetrating tests and vertically-averaged hydraulic properties continue as the basis for dealing with contaminant migration problems, while vertically distributed information is much more vital to successful remediation and meaningful simulation of contaminant transport in aquifers.

Although the use of this layered approach to ground-water hydrology is less restrictive than its vertically averaged counterpart, there are still serious limitations to the complete characterization of the three dimensional variations that actually exist. Errors will exist when analyzing any test, and discrepancies will arise when different tests and different methods are compared.

The results of this investigation suggest that the best strategy for suppressing such errors and discrepancies consists of using an impeller meter to obtain a dimensionless K/$\overline{K}$ distribution, and then a standard pumping test, or a slug test, to compute $\overline{K}$. Combining both types of information enables one to "fit" an impeller meter test to a given aquifer and to obtain dimensional values for K(z). Shown in Figure I-5 is the type of information that results when the two testing procedures are combined.

In the flowmeter applications at Mobile, a different K(z)/$\overline{K}$ distribution was obtained at every vertical scale of measurement at each of seven different wells. As one would expect, the smaller the vertical scale of measurement the larger the degree of apparent heterogeneity. The results of this work suggest that a proper rule of thumb would be to use measurement intervals of about one tenth of the aquifer thickness [Molz et al., 1989b]. However, once the equipment is in place, one foot measurement intervals would be practical in most aquifers. In this way, combinations of data points could be used if at a later date more detailed information becomes desireable, as in the use of some promising new approaches in geostatistics.

CHAPTER II

MULTILEVEL SLUG TESTS FOR MEASURING HYDRAULIC CONDUCTIVITY DISTRIBUTIONS

II-1 INTRODUCTION

As discussed in Appendix I, the impeller meter test is generally superior to the multilevel slug test because the latter requires the hydraulic isolation of a portion of the test aquifer using a straddle packer. However, if reasonable isolation can be achieved the multilevel slug test is a viable procedure for measuring K(z). All equipment needed for such testing is available commercially and the procedure does not require the addition or withdrawal of water to change the head in the well.

The testing apparatus used for the applications reported here are illustrated in Figure II-1. Two inflatable packers separated by a length of perforated, galvanized steel pipe comprised the straddle packer assembly. The length of aquifer sampled by the straddle packer is L=3.63 ft. (1.1 m). A larger packer, referred to as the reservoir packer, is attached to the straddle packer with 2" (5.08 cm) Triloc PVC pipe, creating a unit of fixed length of approximately 100 ft (30.5 m) which can be moved with an attached cable to desired positions in the well. When inflated, the straddle packer isolates a desired test region of the aquifer and the reservoir packer isolates a reservoir in the 6" (15.2 cm) casing above the multilevel slug test unit and below the potentiometric surface of the confined aquifer.

An advantage of this design is that the 2 in (5.08 cm) connecting pipe, and other factors contributing to head losses, remains unchanged regardless of packer elevation in the well. The inflatable lengths of the straddle packers are 24.5 in. (62.2 cm) (model 36, pneumatic packer, Tigre Tierra, Inc.) and 39.0 in. for the reservoir packer (99.1 cm) (model 610, pneumatic packer, Tigre Tierra, Inc.)

II-2 PERFORMANCE OF MULTILEVEL SLUG TESTS

Multilevel slug tests are described for three wells (E3, E6, E7) at the Mobile, Alabama site shown in Figure II-2. The wells, formerly used as multilevel tracer sampling wells (Molz, et al. 1988), were constructed of 130 ft of 6 in (15.2 cm) PVC casing to the top of the medium sand aquifer. Fully slotted 4 in (10.2 cm) PVC pipe extended an additional 70 ft (21.3 m) through the aquifer. Well E3 was an exception, having 3 ft (0.91 m) slotted pipe sections separated by 7 ft (2.13 m) solid sections through the aquifer.

In a typical test, water is displaced in the reservoir above the packer. This head increase induces flow through the central core of the reservoir packer and the TriLoc pipe to the straddle packer assembly, then through the slotted well screen into the test region of the aquifer.

In a falling head slug test, an inserted plunger displaces a volume of water in the reservoir creating a depth variation, y=y(t), relative to the initial potentiometric surface. In the same way, a plunger withdrawal is used to create a rising head test. Head measurements are made with a manually operated recorder (Level Head model LH10, with a 10 psig pressure transducer, In Situ, Inc.).

The results of a series of tests at different elevations in well E6 are shown in Figure II-3. The data result from plunger insertion tests where a sudden reservoir depth increase of about y_o=3 ft (0.91 m) was imposed. Depth reduction, y=y(t), which is nearly an exponential decay, is a result of flow into the aquifer test section adjacent to the straddle packer. The different slopes of the straight line approximations (least squares fits) express the variability of hydraulic conductivity in the aquifer at the different test section elevations. Tests repeated at a given elevation were generally reproducible, as shown in Figure II-4, with the maximum difference in slopes being 10% or less.

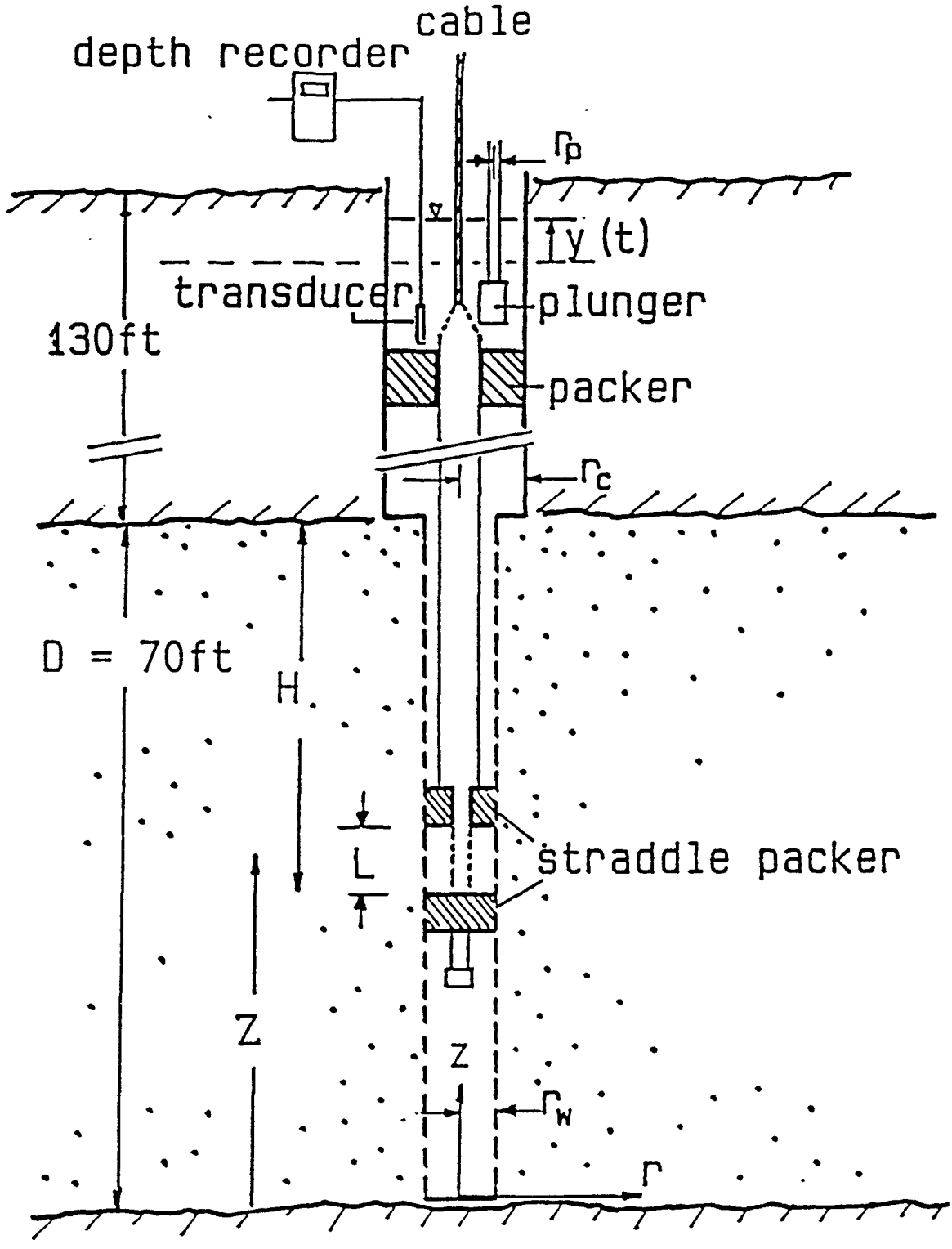

Figure II-1. Schematic Diagram of the Apparatus for Performing a Multilevel Slug Test.

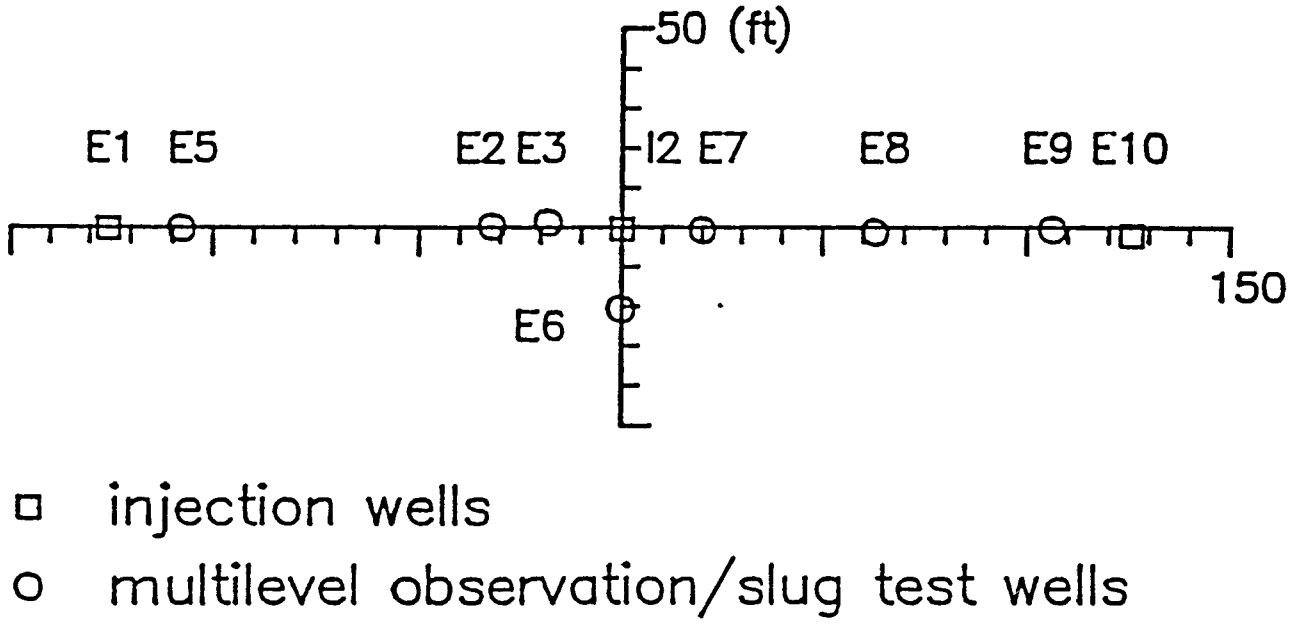

Figure II-2. Plan View of Part of the Well Field at the Mobile Site.

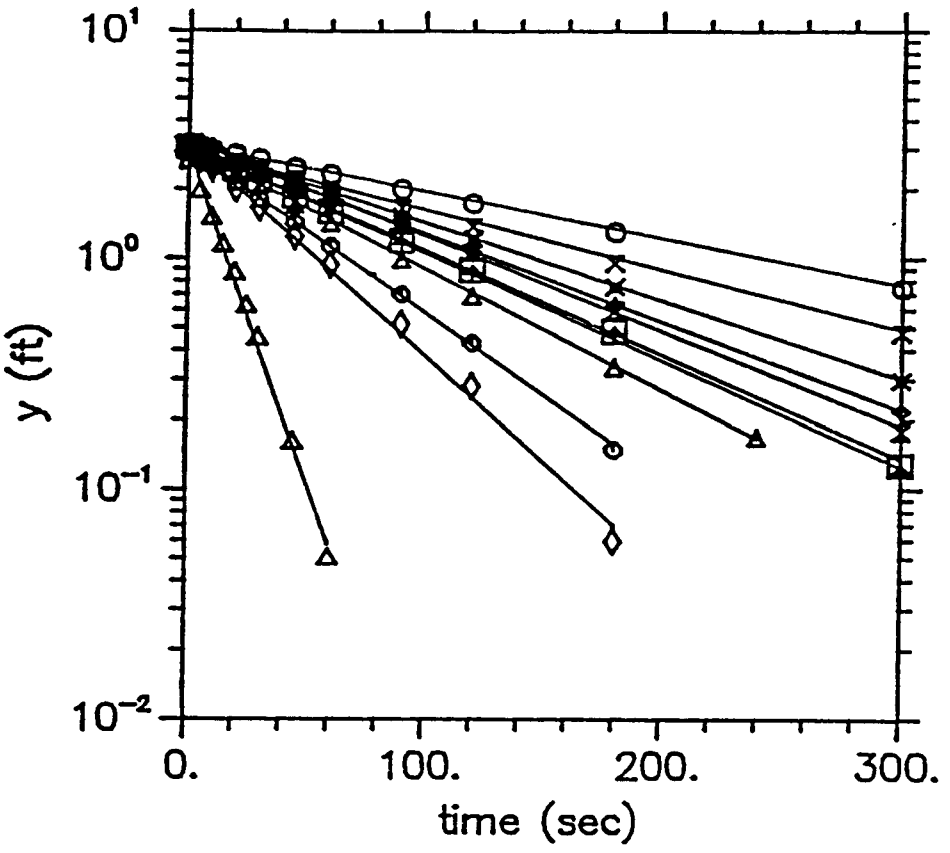

log(y)=−0.0280t+0.47 Z=11.2 ft
log(y)=−0.0045t+0.49 Z=17.2 ft
log(y)=−0.0020t+0.50 Z=23.2 ft
log(y)=−0.0038t+0.49 Z= 5.2 ft
log(y)=−0.0041t+0.51 Z=29.2 ft
log(y)=−0.0034t+0.49 Z=35.2 ft
log(y)=−0.0026t+0.47 Z=41.2 ft
log(y)=−0.0046t+0.48 Z=47.2 ft
log(y)=−0.0053t+0.48 Z=53.2 ft
log(y)=−0.0071t+0.47 Z=59.2 ft
log(y)=−0.0092t+0.50 Z=65.2 ft

Figure II-3. Multilevel Slug Test Data from Well E6. $B=\log(y_1/y_2)/(t_2-t_1)$ = Magnitude of the Slope of the log y(t) Response.

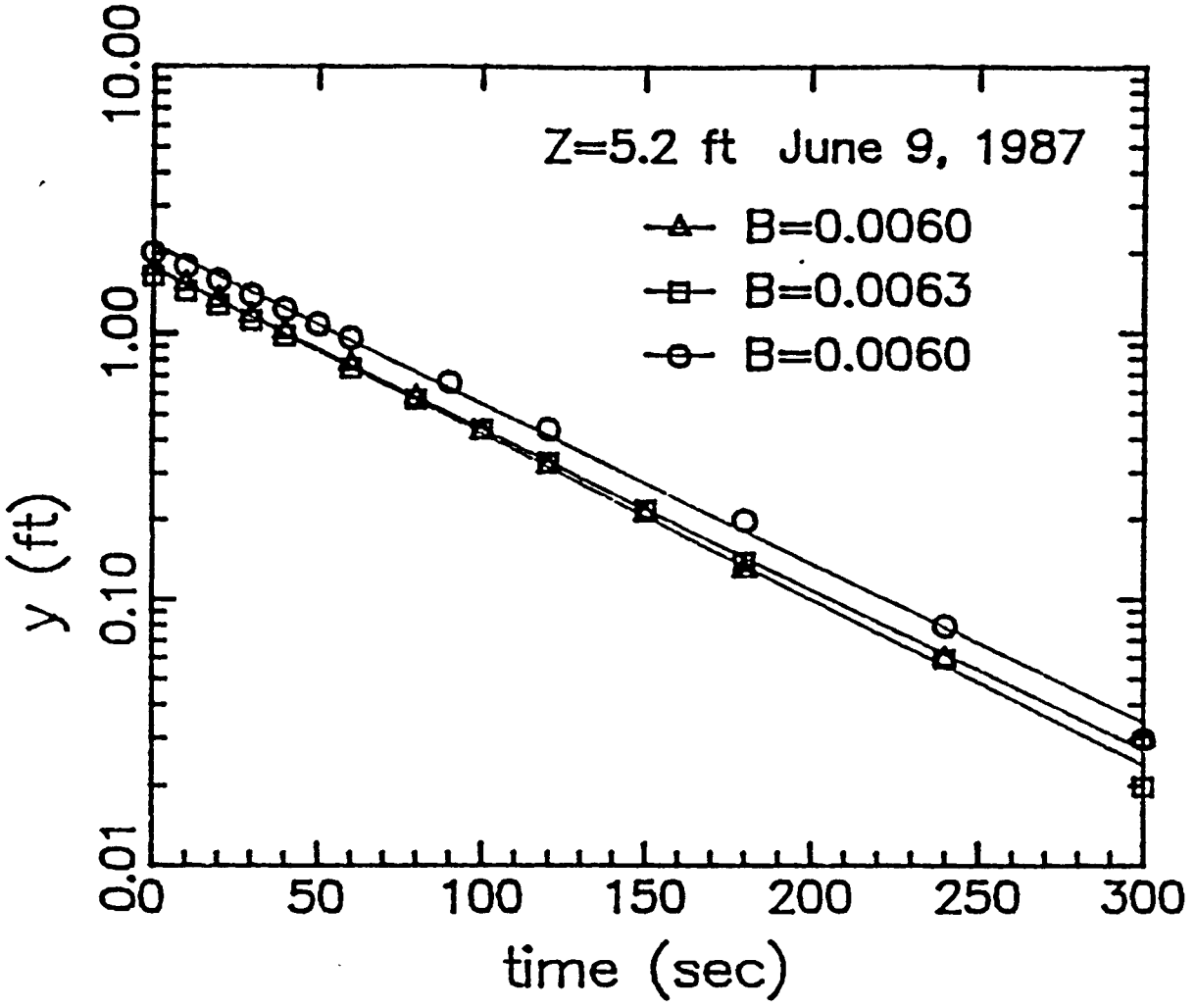

Figure II-4. Plot Showing the Reproducibility of Data Collected at Well E6.

An exception to the general rule of reproducible behavior was observed in well E6. Shown in Figure II-5 are the results of tests at two elevations conducted on three different days. For the July 20 tests, the well had been undisturbed for approximately 40 days. For the July 21 tests it was developed by repeated air injection and flushing prior to the slug testing. Noting the significant change, particularly for the curves having larger slopes, the tests were repeated on July 30 after more extensive development. Since the third set of data was in close agreement with the second, it was concluded that the development was sufficient. This behavior was not observed at other test wells; however, all tests were done after a small amount of redevelopment. The construction of well E6, originally done for tracer observations (Molz, et al., 1986a, 1986b), was intended to minimally disturb the aquifer close to the screen. In these cases, particularly after the passage of several months, minor redevelopment may be required prior to hydraulic testing as clay and silt materials tend to migrate into the well, coating the screen and often collecting at the well bottom.

Multilevel slug testing will be meaningful only if the straddle packer system hydraulically isolates a segment of the screen and the adjacent aquifer. Channels, which will negate the packer seal, may be present between the screen and the borehole. Similarly, backfill material of greater permeability than the formation can allow flow to bypass the packers rather than flowing into the test section. Additional pressure monitoring above and below the straddle packer assembly may be desirable if these types of problems are suspected (Taylor et al., 1989).

II-3 ANALYSIS OF MULTILEVEL DATA

There are essentially three techniques for analyzing partially penetrating slug tests which account for both radial and vertical flow in an aquifer assumed to be locally homogeneous and isotropic (Boast and Kirkham, 1971; Bouwer and Rice, 1976; Dagan, 1978). None of these approaches are entirely satisfactory, especially for test sections that have relatively large diameter to length ratios (Melville et al., 1989; Widdowson et al., 1989). Therefore, there is a need for a more general approach that is reasonably accurate, free from limiting assumptions and easy to use. In addition, it is desirable to have a procedure that includes the effect of anisotropy in the test aquifer since this physical phenomenon is not uncommon.

The purpose of the remainder of this chapter is to present details of a procedure for analyzing slug test data which considers radial and vertical, anisotropic, and axi-symmetric flow to or from a test interval. It is based on a finite element model called EFLOW, licensed through the Electric Power Research Institute and modified at Auburn University.

II-3.1 Mathematical Model Development

Equation II-1 is the mathematical model used in developing the data analysis procedure. Diagrams of the two-dimensional geometry within which the mathematical model is applied are shown in Figure II-6. Diagram (A) applies specifically to a confined aquifer while diagram (B) applies to the unconfined case. When analyzing a partially penetrating slug test in an unconfined aquifer one assumes that the water table stays at a constant elevation throughout the test (Dagan, 1978).

In a homogeneous, anisotropic aquifer, the equation governing transient, axi-symmetric flow is given by:

$$S_s \frac{\partial h}{\partial t} = K\left(\frac{\partial^2 h}{\partial r^2} + \frac{1}{r}\frac{\partial h}{\partial r}\right) + K_z \frac{\partial^2 h}{\partial z^2} \qquad \text{(II-1)}$$

where S_s is specific storage, h is hydraulic head, t is time, r is radial distance, z is vertical distance, and K and K_z are hydraulic conductivities in the radial and vertical directions respectively. The initial and boundary conditions for simulating a slug test within the geometry of Figure II-6 are:

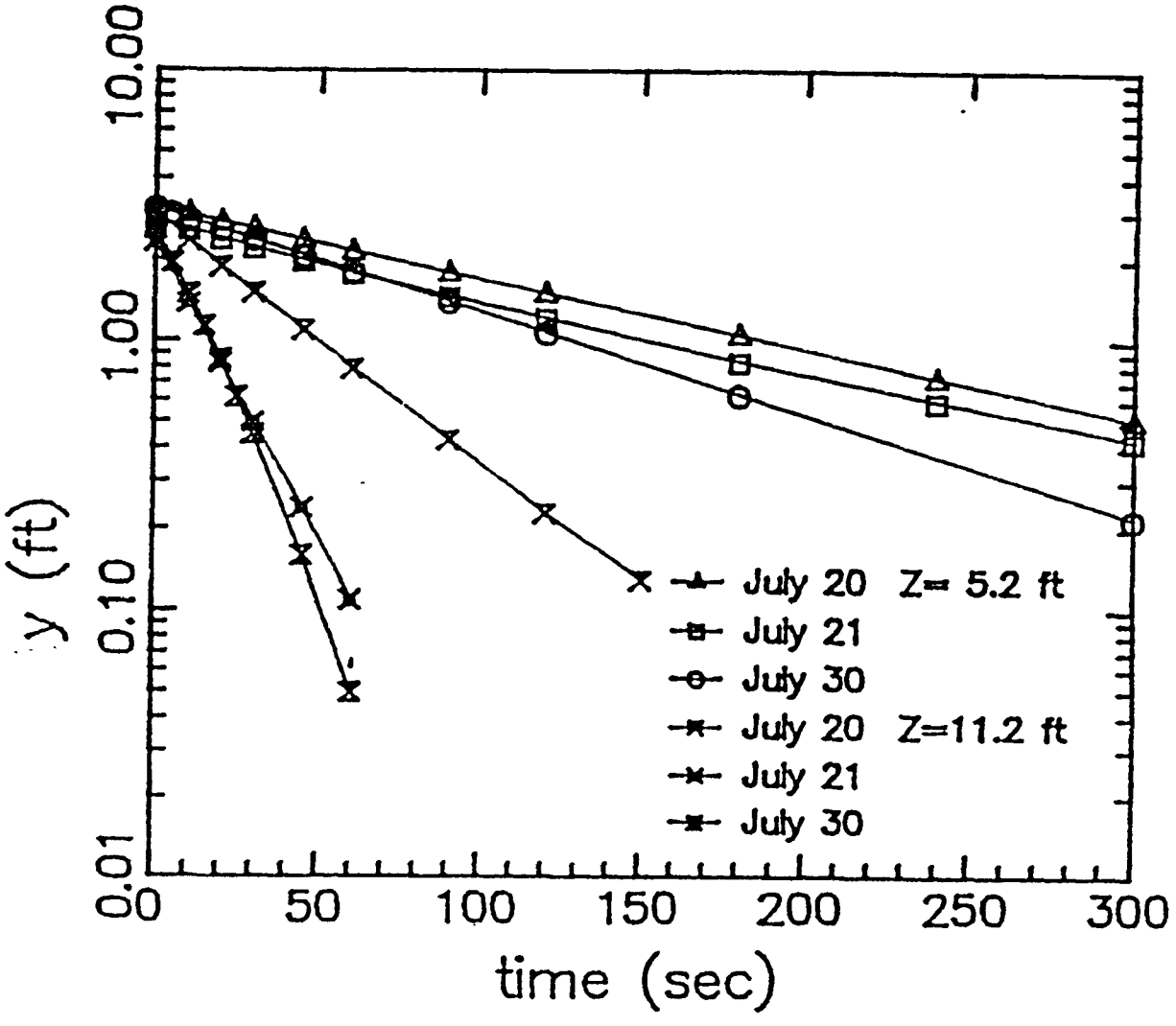

Figure II-5. Plots Showing the Influence of Well Development at Two Elevations in Well E6.

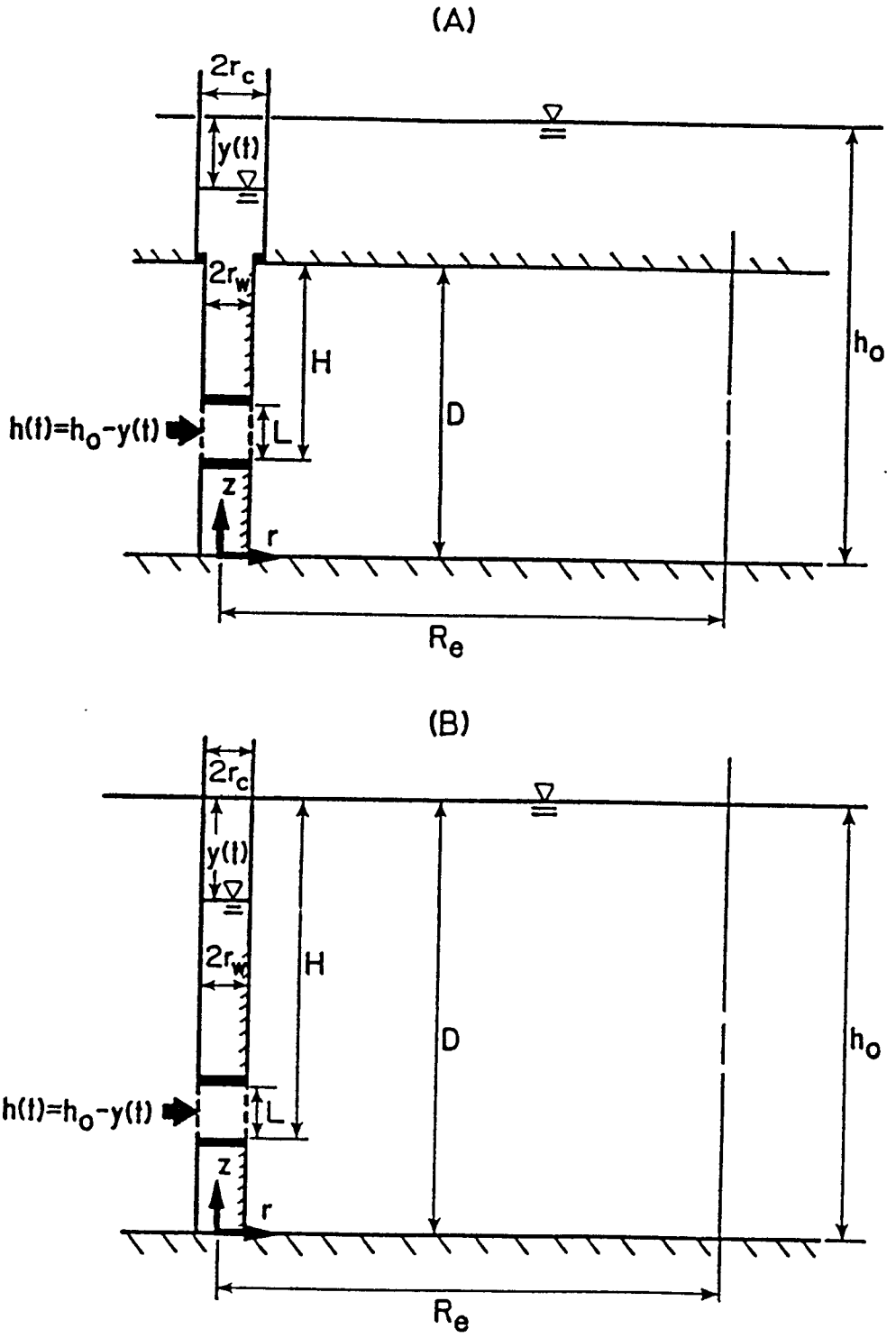

Figure II-6. Diagram Illustrating the Geometry in which a Partially Penetrating Slug Test is Analyzed. Diagram (A) is for the Confined Case and Diagram (B) is for the Unconfined Case.

I.C.) $h(r, z, 0) = h_o$ (II-2)

B.C.) $h(r_w, z, t) = h_o - y(t)$, for $(D-H) \le z \le (D-H+L)$ (II-3)

$$\frac{\partial h}{\partial z}(r, 0, t) = \frac{\partial h}{\partial z}(r, D, t) = 0, \text{ for } r_w < r < R_e \quad \text{(II-4)}$$

$$\frac{\partial h}{\partial r}(r_w, z, t) = 0, \text{ for } 0 \le z < (D-H) \text{ and } (D-H+L) < z < D \quad \text{(II-5)}$$

$h(R_e, z, t) = h_o$, for $0 \le z \le D$ (II-6)

For simulating a partially penetrating slug test in an unconfined aquifer, all boundary and initial conditions remain the same except condition (II-4) which is changed to:

$$\frac{\partial h}{\partial z}(r, 0, t) = 0; \; h(r, D, t) = h_o, \text{ for } r_w < r < R_e \quad \text{(II-7)}$$

It is generally assumed in analyzing a slug test that storage effects are small because of the small volumes of water that are involved (Dagan, 1978). Moreover, the analysis procedure being developed uses as input the slope of the straight-line portion of a plot of log (y(t)) vs. t, and the slope will be constant only after transient storage effects have died out. Since the value of this slope will be independent of S_s, it is sufficient to solve the mathematical model given by:

$$0 = K\left(\frac{\partial^2 h}{\partial r^2} + \frac{1}{r}\frac{\partial h}{\partial r}\right) + K_z \frac{\partial^2 h}{\partial z^2} \quad \text{(II-8)}$$

and subject to the boundary conditions presented previously. This is called a quasi-steady state model because time, which does not appear explicitly in equation (II-8), enters the overall problem due to the time-dependent boundary condition given by (II-3).

II-3.2 Model Solution and Parametric Study

For the specific parameters represented in Figure II-1, the quasi-steady flow model was solved using EFLOW. A representative set of solutions was obtained for each anisotropy ratio of interest for both confined and unconfined conditions. The dependence of each solution on various parameters such as K, H, L, and r_w, was summarized using the dimensionless variable plots suggested by Dagan (1978). The possible dependence of each solution on R_e (radius of influence) was removed by choosing a sufficiently large value so that large perturbations about this value had a negligible effect on the numerical solution. The reasoning behind the parametric study is given below.

By conservation, the rate of change of the test well water level (Fig. II-6) with respect to time, dy/dt, is related to the volumetric flow rate into the aquifer, Q, by:

$$Q = -A_c(dy/dt) \quad \text{(II-9)}$$

where A_c is the cross-section area of the casing. A_c will depend on the radius of the casing and the cross-sectional area of items in the casing causing displacement.

For a given set of aquifer conditions at steady state, flow into the aquifer is proportional to y; that is, a doubling y will double the flow. More precisely:

$$Q = \beta y \quad \text{(II-10)}$$

where β is the constant of proportionality. Combining equations (II-9) and (II-10) yield:

$$(1/y)dy/dt = d(\ln(y))/dt = -\beta/A_c \quad \text{(II-11)}$$

Since the right-hand side of (II-11) is constant, a plot of ln(y) versus t must be linear.

Through the use of Darcy's law the flow into the aquifer may also be expressed as:

$$Q = 2\pi r_w K \int_{D-H}^{D-H+L} \frac{\partial h}{\partial r} (r_w,z)dz \qquad \text{(II-12)}$$

A dimensionless flow parameter, P, can now be defined as:

$$P = \frac{Q}{2\pi KLy} = \frac{r_w}{Ly} \int_{D-H}^{D-H+L} \frac{\partial h}{\partial r} (r_w,z)dz \qquad \text{(II-13)}$$

The parameter, P, depends only on the configuration of a particular slug test. From numerical solutions of equation (II-8) for different configurations of Figure II-1, and using equation (II-13), Figures II-7 and II-8 were generated for confined and unconfined cases showing the dependence of P on H/L and L/r_w for isotropic conditions. Also, dimensionless data for K/K_z ratios of 1, 0.2 and 0.1 are presented in Tables II-1 through II-6.

Once the various figures or tables are developed for a given anisotropy ratio, they may be used in combination with a semi-log plot of slug test data to calculate the hydraulic conductivity in the radial direction. For example, from Fig. II-7 the appropriate values of H/L, and L/r_w can be used to obtain P (call it P_n). Then, using equation (II-9) one notes that:

$$Q = 2\pi KLyP_n = - A_c(dy/dt) \qquad \text{(II-14)}$$

Using the relationship $(1/y)dy/dt = d(\ln(y))/dt$ and solving equation (II-14) for K yields:

$$K = -\frac{A_c}{2\pi LP_n} \frac{d(\ln(y))}{dt} = -\frac{A_c}{2\pi LP_n}(2.3B) \qquad \text{(II-15)}$$

where B is the slope of a semi-log plot (base 10 logs) of y vs. t, with the y vs. t values obtained from an actual slug test. B should always be considered a negative number regardless of whether y is above or below the reference level during the slug test.

II-3.3 Numerical Example

Multilevel slug test data from the Mobile site has been analyzed using the method presented here (Melville et al., 1989). Data from eleven levels in a test well are shown in Figure II-3 along with straight line representations using linear regression. The following applies specifically to the data centered at z=11.2 ft where $A_c = 0.180$ ft^3. The procedure by which the individual hydraulic conductivity values can be calculated is:

1. Obtain a measurement or estimate of aquifer anisotropy ratio.

   $K:K_z = 6.7:1$. (Parr et al., 1983)

2. Calculate H/L and $\log(L/r_w)$ from experimental geometry.

   Aquifer thickness, D = 70 ft

   Packer separation length, L = 3.63 ft

   Distance (H) to closest boundary = 13.01 ft

   Radius of screen = 0.167 ft

H/L= 3.58

L/r_w = 21.8; $\log_{10}(L/r_w)$ = 1.34

3. Select dimensionless discharge by interpolating between 1:5 and 1:10 anisotropy values in Tables II-2 and II-3.

P_n = 0.277

4. Determine slope of semi-log data plot (Figure II-3).

B = 0.028 sec^{-1}

5. Calculate hydraulic conductivity from equation (II-15).

K = 0.00183 ft/sec = 158 ft/day

If an average hydraulic conductivity, $\overline{K}$, is available from full aquifer pumping tests, multilevel tests like those described here could be used to develop $K(z)/\overline{K}$ profiles. This method of obtaining K(z) profiles to assist in the characterization of contaminant transport appears to be practical under the proper conditions.

There can be serious reservations about the reality of slug test data; however, those tests performed in wells having slotted screens at the Mobile site appear to be reasonably accurate. It was not possible to perform slug tests in wells having wire-wrapped screens because of vertical leakage in the screen structure that could not be prevented with packers. As discussed in Braester and Thunvik (1984), partially-penetrating slug tests are very sensitive to cylindrical annuli of high or low permeability surrounding a well; therefore, gravel or sand filter pack should never be used. Tests in unscreened boreholes are questionable because the surface of the formation can become coated with low permeability materials.

These restrictions make multilevel slug testing much more problematical than impeller meter testing. However, if the formation permeability is sufficiently low to prevent the use of an impeller meters, because of stall speed problems, multilevel slug testing may be a viable alternative.

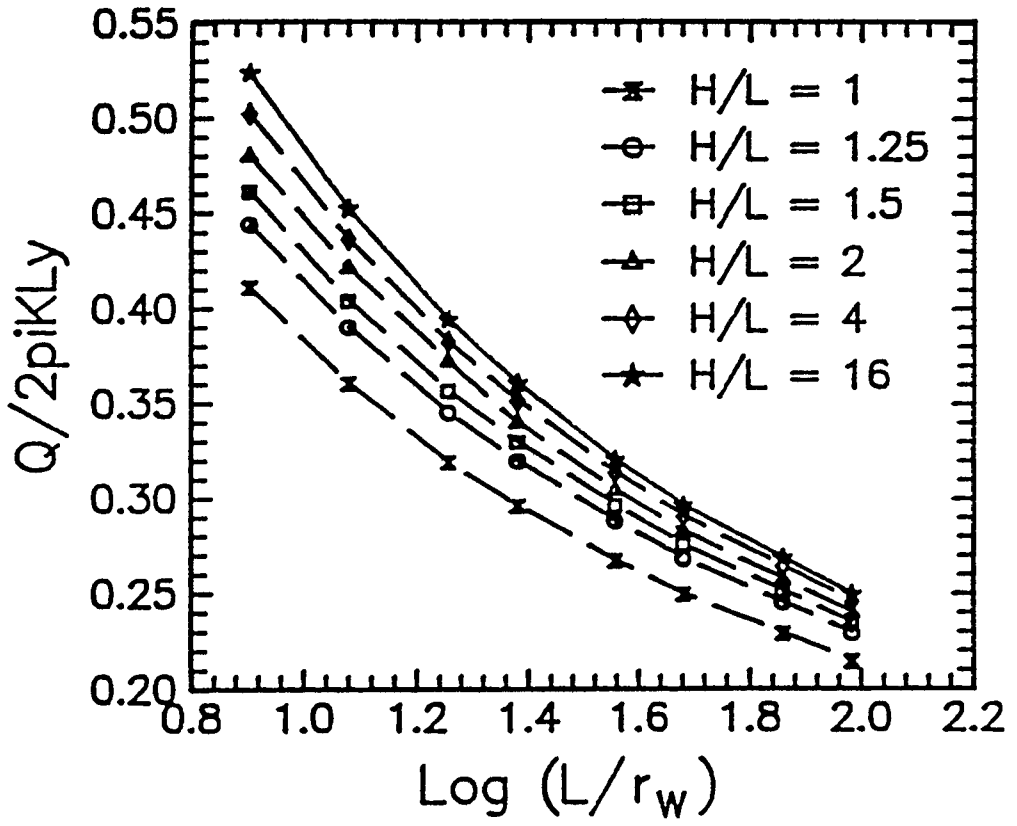

Figure II-7. Plots of Dimensionless Discharge, P = Q/2πKLy, for the Isotropic, Confined Aquifer Problem as a Function of L/r_w And H/L.

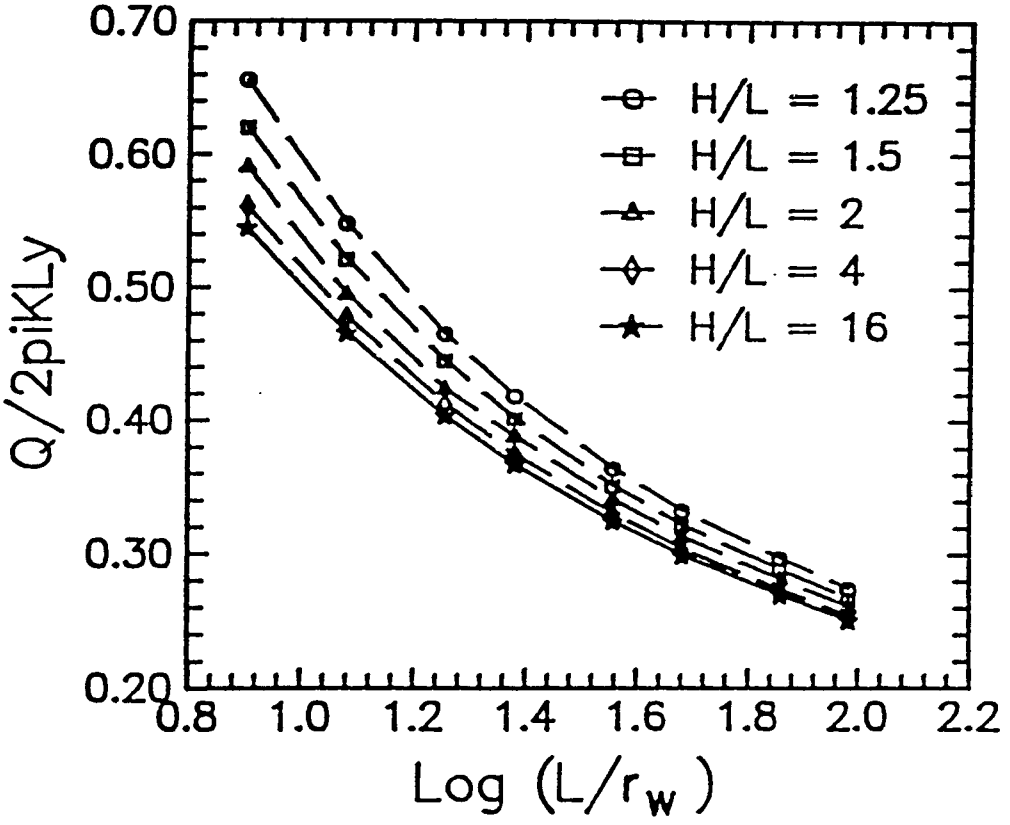

Figure II-8. Plots of Dimensionless Discharge, $P = Q/2\pi KLy$, for the Isotropic, Unconfined Aquifer Problem as a Function of L/r_w and H/L.

TABLE II-1. DIMENSIONLESS DISCHARGE, P, AS A FUNCTION OF H/L AND L/r_w FOR THE CONFINED CASE WITH K/K_z = 1.0.

L/r_w =	8	12	18	24	36	48	72	96
H/L								
1	.4117	.3610	.3196	.2964	.2675	.2497	.2293	.2147
1.25	.4448	.3905	.3456	.3202	.2882	.2685	.2455	.2295
1.5	.4617	.4045	.3570	.3303	.2965	.2757	.2515	.2348
2	.4805	.4219	.3725	.3402	.3045	.2828	.2575	.2400
4	.5029	.4370	.3829	.3519	.3140	.2908	.2645	.2459
8	.5155	.4463	.3898	.3576	.3183	.2945	.2674	.2484
16	.5243	.4526	.3945	.3610	.3207	.2964	.2687	.2496

TABLE II-2. DIMENSIONLESS DISCHARGE, P, AS A FUNCTION OF H/L AND L/r_w FOR THE CONFINED CASE WITH K/K_z = 0.2.

L/r_w =	8	12	18	24	36	48	72	96
H/L								
1	.3205	.2874	.2597	.2434	.2230	.2102	.1955	.1847
1.25	.3428	.3076	.2778	.2601	.2377	.2238	.2078	.1957
1.5	.3533	.3165	.2852	.2667	.2434	.2288	.2124	.1997
2	.3660	.3279	.2950	.2741	.2487	.2336	.2168	.2034
4	.3771	.3360	.3013	.2806	.2551	.2392	.2215	.2076
8	.3837	.3411	.3053	.2840	.2577	.2415	.2232	.2092
16	.3878	.3442	.3076	.2858	.2589	.2424	.2237	.2096

TABLE II-3. DIMENSIONLESS DISCHARGE, P, AS A FUNCTION OF H/L and L/r_w FOR THE CONFINED CASE WITH K/K_z = 0.1.

L/r_w =	8	12	18	24	36	48	72	96
H/L								
1	.2914	.2634	.2398	.2256	.2078	.1966	.1839	.1742
1.25	.3121	.2821	.2567	.2410	.2207	.2085	.1949	.1840
1.5	.3209	.2894	.2630	.2457	.2255	.2129	.1990	.1876
2	.3295	.2979	.2701	.2523	.2302	.2172	.2028	.1909
4	.3401	.3055	.2765	.2588	.2357	.2219	.2068	.1945
8	.3453	.3096	.2798	.2615	.2378	.2238	.2081	.1958
16	.3463	.3105	.2800	.2616	.2387	.2245	.2083	.1960

TABLE II-4. DIMENSIONLESS DISCHARGE, P, AS A FUNCTION OF H/L AND L/r_w FOR THE UNCONFINED CASE WITH K/K_z = 1.0.

L/r_w =	8	12	18	24	36	48	72	96
H/L								
1.25	.6564	.5487	.4658	.4186	.3644	.3329	.2973	.2742
1.5	.6207	.5219	.4455	.4018	.3515	.3220	.2887	.2667
2	.5912	.4955	.4241	.3883	.3410	.3132	.2813	.2605
4	.5616	.4783	.4129	.3748	.3305	.3042	.2736	.2540
8	.5505	.4701	.4066	.3697	.3264	.3007	.2707	.2516
16	.5453	.4662	.4036	.3672	.3244	.2990	.2695	.2505

TABLE II-5. DIMENSIONLESS DISCHARGE, P, AS A FUNCTION OF H/L AND L/r_w FOR THE UNCONFINED CASE WITH K/K_z = 0.2.

L/r_w =	8	12	18	24	36	48	72	96
H/L								
1.25	.4528	.3944	.3469	.3187	.2853	.2651	.2423	.2258
1.5	.4351	.3802	.3356	.3090	.2774	.2582	.2362	.2206
2	.4201	.3683	.3256	.3018	.2708	.2524	.2311	.2162
4	.4047	.3564	.3166	.2926	.2639	.2463	.2259	.2117
8	.3988	.3517	.3128	.2894	.2612	.2441	.2242	.2102
16	.3960	.3494	.3110	.2879	.2601	.2431	.2238	.2097

TABLE II-6. DIMENSIONLESS DISCHARGE, P, AS A FUNCTION OF H/L AND L/r_w FOR THE UNCONFINED CASE WITH K/K_z = 0.1.

L/r_w =	8	12	18	24	36	48	72	96
H/L								
1.25	.3960	.3498	.3114	.2883	.2605	.2434	.2237	.2096
1.5	.3824	.3386	.3023	.2804	.2539	.2376	.2185	.2051
2	.3724	.3292	.2946	.2737	.2482	.2326	.2141	.2012
4	.3587	.3195	.2867	.2667	.2424	.2274	.2098	.1974
8	.3540	.3157	.2835	.2640	.2402	.2255	.2085	.1962
16	.3517	.3139	.2821	.2628	.2393	.2248	.2083	.1960

CHAPTER III

CHARACTERIZING FLOW PATHS AND PERMEABILITY DISTRIBUTIONS IN FRACTURED ROCK AQUIFERS*

III-1 INTRODUCTION

In chapters I and II, the impeller meter test and the multilevel slug test were described as a means for measuring vertical hydraulic conductivity distributions. This chapter deals with the application of the borehole heat-pulse flowmeter. It can be used as an alternative to an impeller flow meter in virtually any application because of its greater sensitivity. This increased sensitivity is particularly important near the bottom of test wells where flow velocities are small.

Spinner flowmeters are limited to minimum velocities of about 3 to 10 ft/min (1 to 3 m/min) allowing flow volumes of as much as 4 gal/min (15 l/min) to go undetected in a 4-in (10 cm) diameter borehole. However, impeller flowmeters are available commercially while heat-pulse flowmeters are in a developmental stage.

Since the analysis of data obtained with a heat-pulse flowmeter in granular aquifers is identical to that discussed for impeller meter data this chapter will be devoted to the application of flowmeters, particularly heat-pulse flowmeters, to fractured rock aquifers. Such meters may be used to locate productive fracture zones and to characterize apparent hydraulic conductivity distributions. Because flow from or into individual fractures is often small, flowmeters more sensitive than impeller meters are commonly needed.

Several thermal flow-measuring techniques have been developed for the measurement of slow flows, including a thermal flowmeter described by Chapman and Robinson (1962) and an evaluation of hot-wire and hot-film anemometers by Morrow and Kline (1971). Dudgeon et al. (1975) reported the development of a heat-pulse flowmeter that uses a minimal-energy thermal pulse in a tag-trace, travel-time technique which is only 1.63 in (41 mm) in diameter and can be used in small-diameter boreholes. Although other thermal flowmeters considered have not proved to be practical in a borehole environment, the commercial version of the Dudgeon style heat-pulse flowmeter was determined to be viable even though it lacks important features; such as seals, which could withstand water pressures to at least 10,000 ft (3,048 m), insensitivity to changes in logging cable resistance and stray electrical currents, and integral centralizers (Hess, 1982).

The basic measurement principle of the USGS Meter is to create a thin horizontal disc of heated water within the well screen at a known time and a known distance from two thermocouple heat sensors, one above and one below the heating element. As the heat pulse moves upward or downward with the water flow, the time required for the temperature peak to arrive at one of the heat sensors is measured. The velocity is then determined by dividing the known travel distance by the time of travel. Thermal buoyancy effects are eliminated by raising the water temperature only a small fraction of a centigrade degree.

This chapter describes three case studies where flow measurements were used to provide a quick survey of aquifer hydraulic responses in fractured rock. They markedly reduce the time required to complete aquifer characterizations using conventional hydraulic tests and tracer studies.

III-2 THE U.S. GEOLOGICAL SURVEY'S THERMAL FLOWMETER

The urgent need for a reliable, slow-velocity flowmeter prompted the USGS to develop a small-diameter, sensitive, thermal flowmeter that would operate to depths of 10,000 ft (3,048 m) or more using 16,000 ft (5,000 m) or longer lengths of conventional four-conductor logging cable (Figure III-1). The thermal flowmeter developed by the U.S.G.S. has interchangeable flow-sensors, 1.63 and 2.5 in. (41 and 64 mm) in diameters, and

---

* Material in this chapter was prepared by Alfred E. Hess and Frederick L. Paillet under sponsorship of the Water Resources Division, U.S. Geological Survey, at the Denver Federal Center, Denver, CO 80225.

has a flow sensitivity from 0.1 to 20 ft/min (0.03 to 6.1 m/min) in boreholes with diameters that range from 2 to 5 in (50 to 125 mm). The vertical velocity in a borehole is measured with the thermal flowmeter by noting the time-of-travel of a heat pulse and using calibration charts developed in the laboratory using a tube with a diameter similar to that of the borehole under investigation (Hess, 1986).

After the thermal flowmeter was tested at several sites, an inflatable, flow-concentrating packer was developed to decrease measurement uncertainties caused by geothermally induced convection currents within the borehole and to increase flow sensitivity in larger diameter holes. The flowmeter and packer have been integrated into a single probe operating on logging lines having four or more conductors (Figure III-2). The assembly can be used with other borehole probes, such as spinner flowmeters and pressure transducers, whose functions are enhanced by the use of an easily controlled packer (Hess, 1988).

The thermal flowmeter, with or without packers, has been used to measure natural or artificially induced flow distributions in boreholes with diameters ranging from 3 to 10 in (75 to 250 mm), at temperatures from 6 to 60°C, and in a variety of lithologies including basalt, dolomite, gneiss, granite, limestone, sandstone, and shale.

With the packer inflated, thermal travel times correlate with borehole flows, rather than vertical velocity, and can detect flows in the range of 0.02 to 2 gal/min (0.04 to 8 L/m). A representative flow calibration chart is shown in Figure III-3 with curves for the packer inflated, deflated, or not installed. The inverse of the time-of-travel is used on the calibration chart for ease and accuracy in reading the curves (Hess, 1982).

The thermal flowmeter was used initially to define naturally occurring flows in boreholes. However, it has been used in additional applications, such as locating fractures that produce water during aquifer tests and identifying flows induced in adjacent boreholes during such tests. The rapid measurement provided by the thermal flowmeter suggests that a few hours of measurements may save days or weeks in investigations using conventional packer and tracer techniques.

III-2.1 Case Study 1--Fractured Dolomite in Northeastern Illinois

Acoustic-televiewer, caliper, single-point-resistance, and flowmeter logs were obtained in a 210 ft (64 m) borehole in northeastern Illinois as part of a study of contaminant migration in fractured dolomite (Figure III-4). The acoustic-televiewer log is a magnetically orientated, pseudo-television image of the borehole wall which is produced with a short-range sonar probe (Zemanek et al., 1970). Irregularities in the borehole wall, such as fracture and vugular openings, absorb or scatter the incident acoustic energy resulting in dark features on the recorded image. Such televiewer logs may be used to determine the strike and dip of observed features (Paillet et al., 1985).

The acoustic-televiewer and caliper logs for borehole DH-14 indicate a number of nearly horizontal fractures which seem to be associated with bedding planes. The largest of these are designated A, B, C, and D in Figure III-4. The caliper log indicates that the major planar features on the televiewer log are large fractures or solution openings associated with substantial borehole diameter enlargements. The large but irregular features between fractures B and C also are associated with borehole enlargements but are interpreted as vugular cavities within the dolomite rather than fractures. The single-point-resistance log indicates abrupt shifts in resistance at depths of about 130 and 185 ft (40 and 56 m) which may reflect differences in the dissolved solids concentration of water in the borehole.

The pattern of vertical flow determined by the flowmeter indicated the probable origin of the water quality contrasts in the borehole (Figure III-4). The flowmeter log indicated downflow, which probably was associated with naturally occurring hydraulic head differences, causing water to enter at the uppermost fracture, A, and exit at fracture B. A much smaller flow, with the same electrical conductivity and dissolved solids concentration, continued down the borehole to fracture C. At this fracture, the downflow increased and flow coming into the well apparently contained a greater concentration of dissolved solids, which accounts for the greater electrical conductivity. This increased downflow exited the borehole at fracture D where there was another, somewhat smaller shift in single-point-resistance. Although not rigorously proven from the geophysical logs, the second shift in resistance appears to be associated with the dissolved solids concentration of the water entering at fracture C.

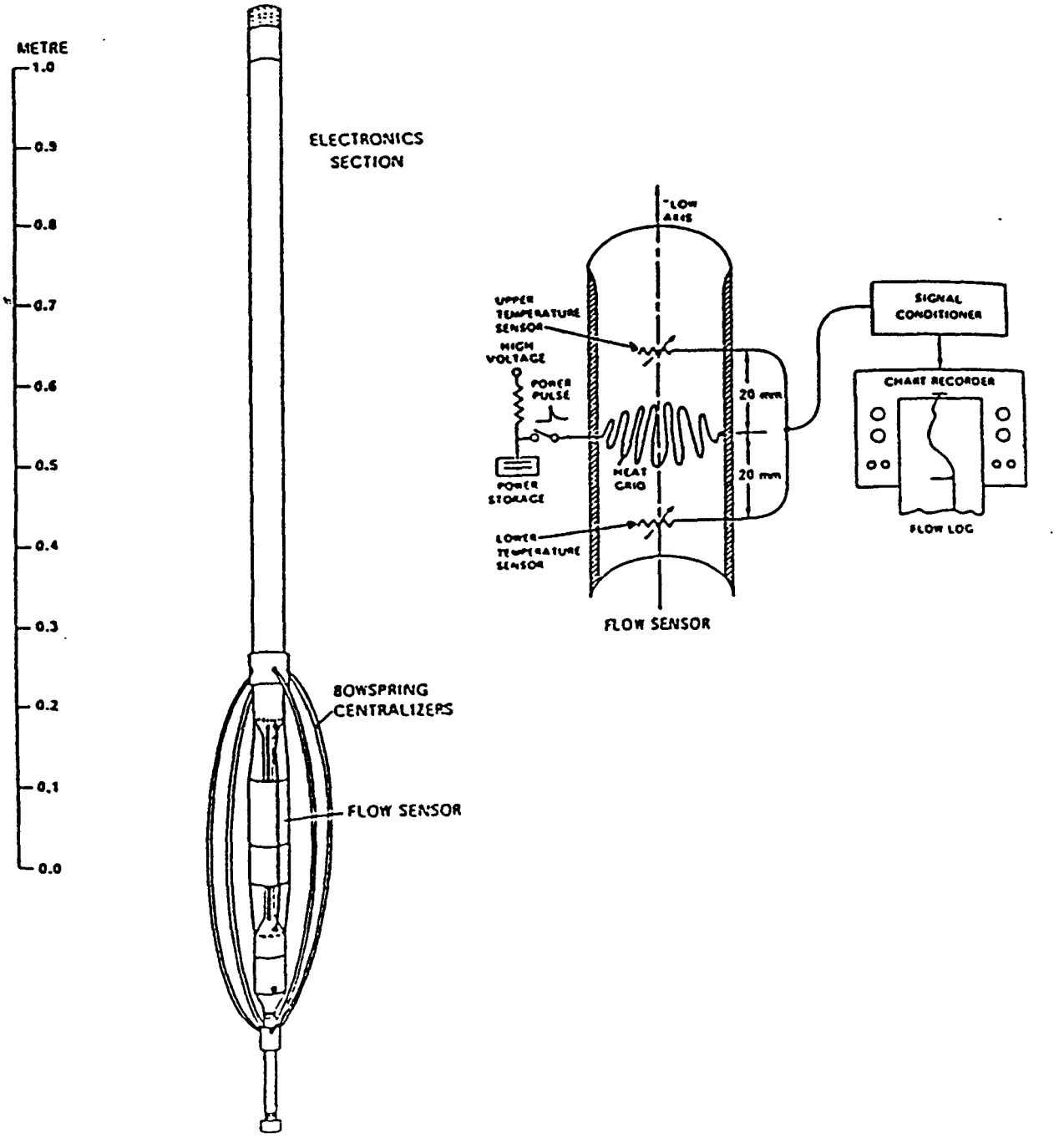

Figure III-1. The U.S. Geological Survey's Slow Velocity Sensitive Thermal Flowmeter (Modified Hess, 1986).

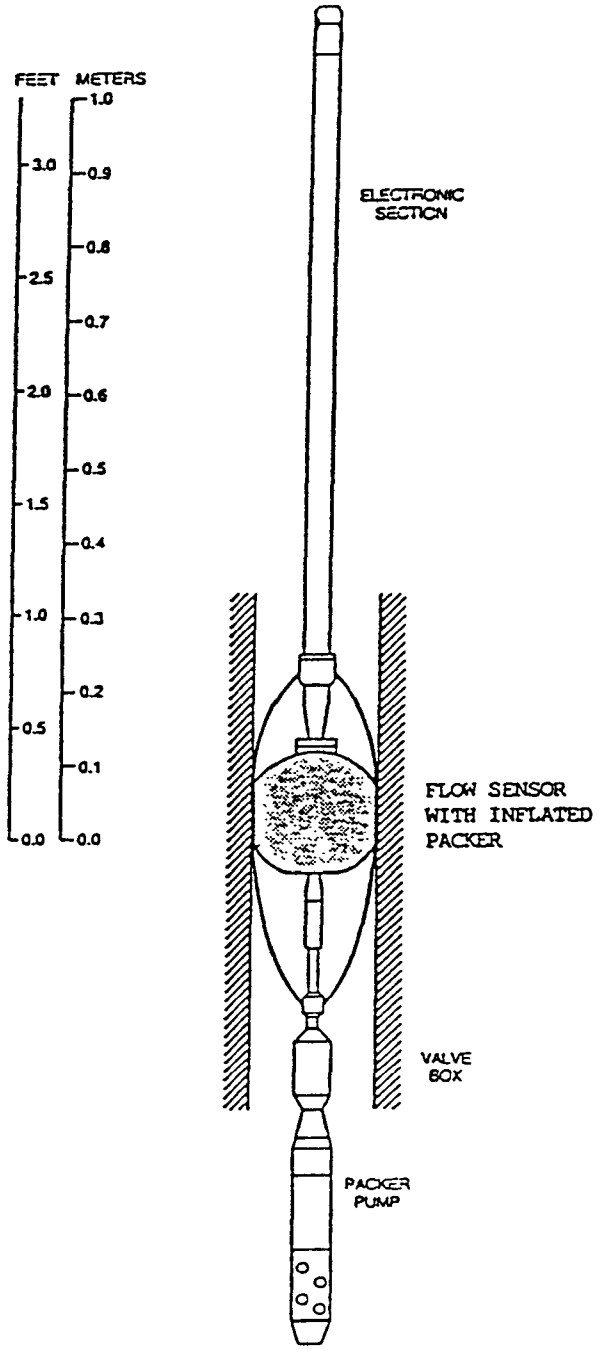

Figure III-2. The U.S. Geological Survey's Thermal Flowmeter with Inflated Flow-Concentrating Packer (Modified Hess, 1988).

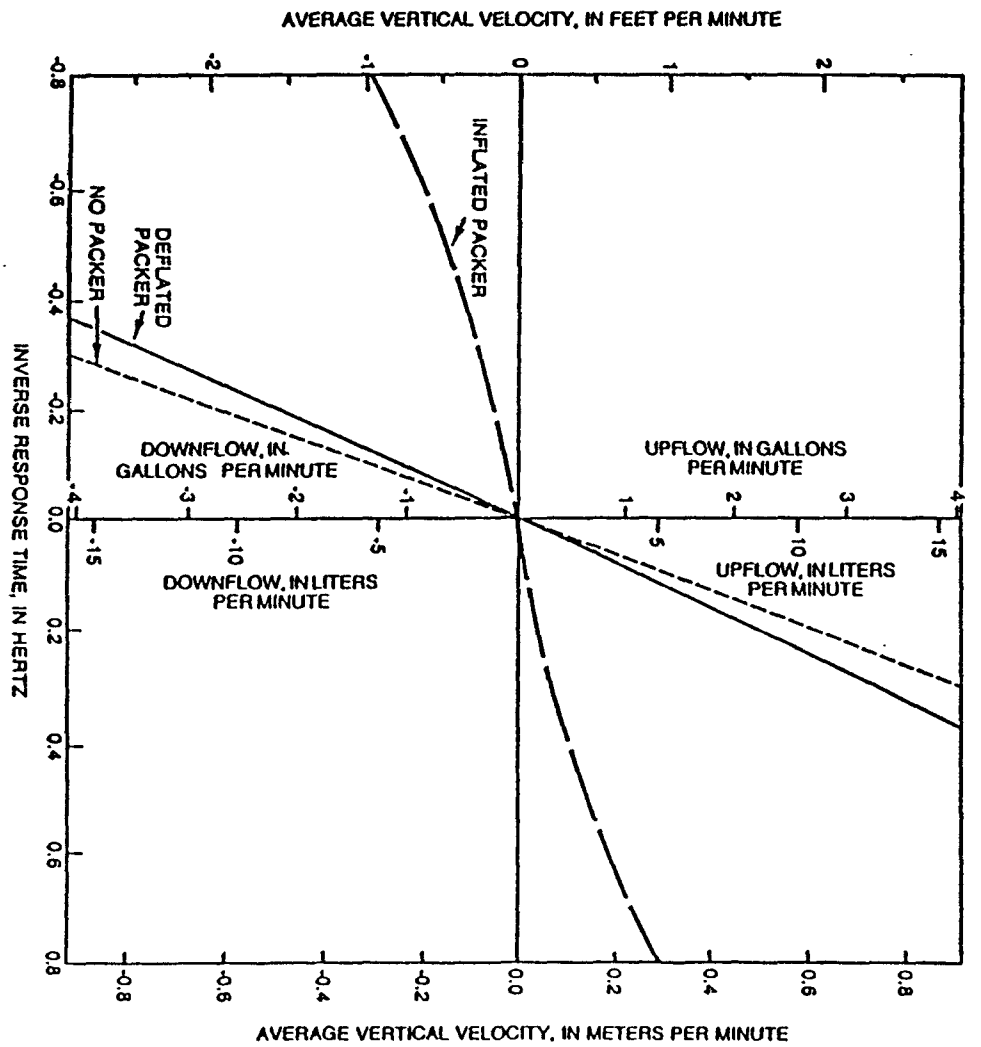

Figure III-3. Example of a Thermal Flowmeter Calibration in a 6-inch (15.2 cm) Diameter Calibration Column.

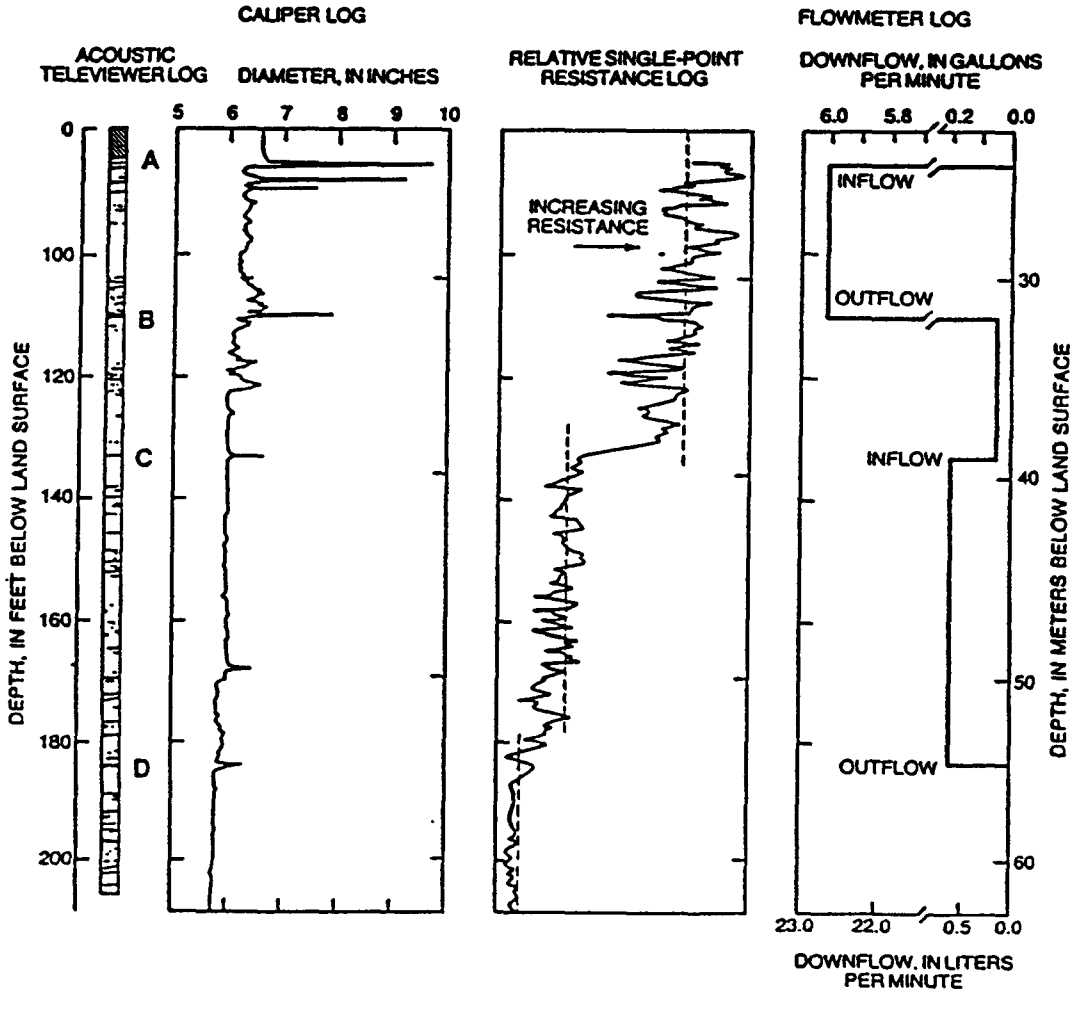

Figure III-4. Acoustic-Televiewer, Caliper, Single-Point Resistance, and Flowmeter Logs for Borehole DH-14 in Northeastern Illinois.

Subsequent water sampling confirmed that there were differences in the dissolved solids concentration of the water at different depths. Sample analysis indicated that the water entering at fracture A had a dissolved solids concentration of about 750 mg/L and that entering at fracture C had a dissolved solids concentration of about 1,800 mg/L. In this instance the geophysical data, especially the thermal-flowmeter data, were useful in planning subsequent packer testing and in interpreting the results of water-quality measurements.

The identification of natural differences in background water quality was useful in modeling the transport of conservative solutes. At the same time, measurements of vertical velocity distributions provided useful indications of hydraulic head differences between different depth intervals. This information could not be obtained from conventional water level measurements without the time consuming installation of packers at multiple levels in all boreholes at the site.

III-2.2 Case Study 2--Fractured Gneiss in Southeastern New York

Conventional geophysical and televiewer logs were obtained in a 400 ft (123 m) borehole completed in fractured gneiss at a contaminated ground-water site in southeastern New York, about 200 ft (70 m) from Lake Mahopac. After a night of recovery from the effects of pumping nearby wells, the water level in the borehole appeared to be slightly higher than the lake level, even though the lake level is generally higher during the day. The acoustic-televiewer log indicated that fractures intersected almost every depth interval of this borehole. Although brine-solution tracing indicated there was downflow within the borehole, the locations of entry and exit points were uncertain.

Acoustic-televiewer and caliper logs for selected intervals of the borehole are shown in Figure III-5. The caliper log indicates several borehole enlargements at point A just below the bottom of the casing and other enlargements, B and C, near the bottom of the borehole. The televiewer log confirmed a large number of major fractures that could be entry and exit points.

Flowmeter logs indicated both the entry and exit points of downflow (Figure III-6). With just a few hours of flowmeter measurements the entry points of the downflow were isolated to the uppermost fractures with most being from fracture A. Consistent differences in the downflow indicated that about 20 percent exited at fracture B and the rest at fracture C.

Flowmeter measurements also indicated a series of transient fluctuations in downward flow which are attributed to the effects of pumping in nearby water-supply wells and the resulting head differences between shallow and deep fractures. The downward flow between fractures A and B was determined to vary from a maximum of about 0.7 gal/min (2.7 L/min) to a minimum of 0.4 gal/min (1.5 L/min) during periods ranging from a few minutes to an hour.

These results enabled hydrologists studying the contamination problem to infer local flow conditions in the aquifer. The results of flowmeter measurements provide useful information about hydraulic head differences between the upper and lower fracture zones and the extent of interconnection between individual fracture sets within those zones. Of special interest is the small proportion of the many large fractures, indicated by the caliper log, that actually produced or accepted flow under ambient hydraulic head conditions. This conclusion agrees with several other recent studies of fractured-rock aquifers (Paillet et al., 1987; Paillet and Hess, 1987).

III-2.3 Case Study 3--Water Movement in and Around a Fracture Zone On The Canadian Shield In Manitoba

This study describes flow in interconnected fractures for an isolated fracture zone on the southeastern margin of the Canadian Shield in Manitoba, Canada. Two boreholes 425 ft (130 m) apart intersected a fracture zone at about 870 ft (265 m). The depths on the logs are somewhat greater than actual vertical depths because the boreholes had been angled deliberately by about 20 degrees. As shown in Figure III-7, the boreholes intersected almost no fractures except those associated with the major zone. The results indicate substantial permeability in the main fracture zone and in several sets of fractures that appear to splay from it.

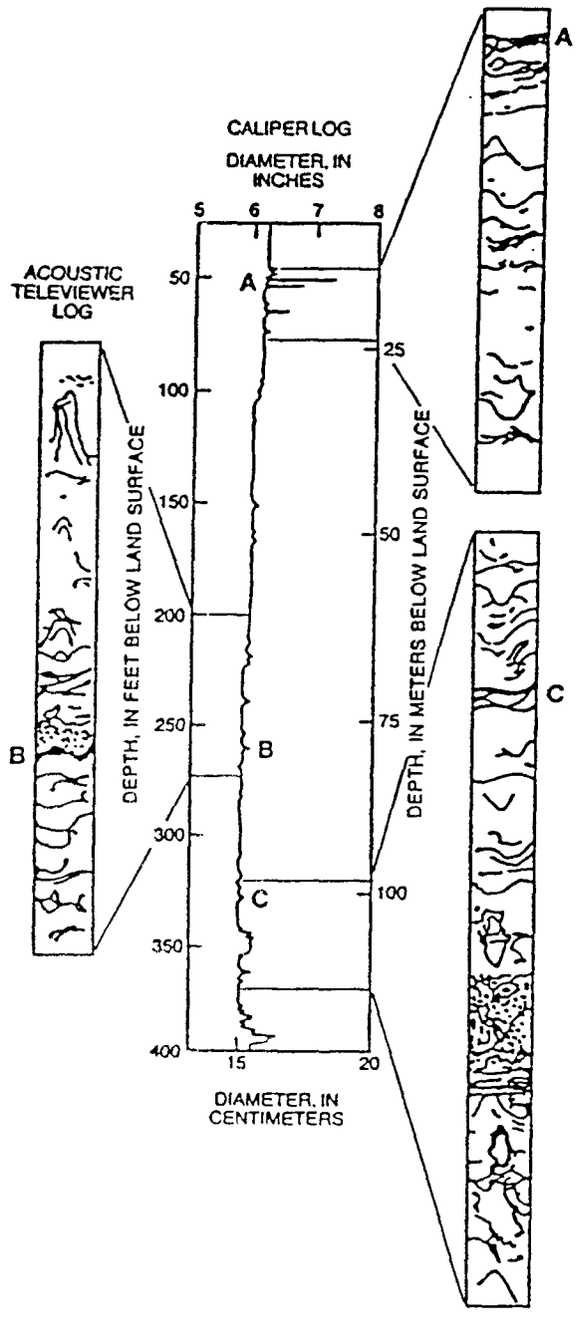

Figure III-5. Acoustic-Televiewer and Caliper Logs for Selected Intervals in a Borehole in Southeastern New York.

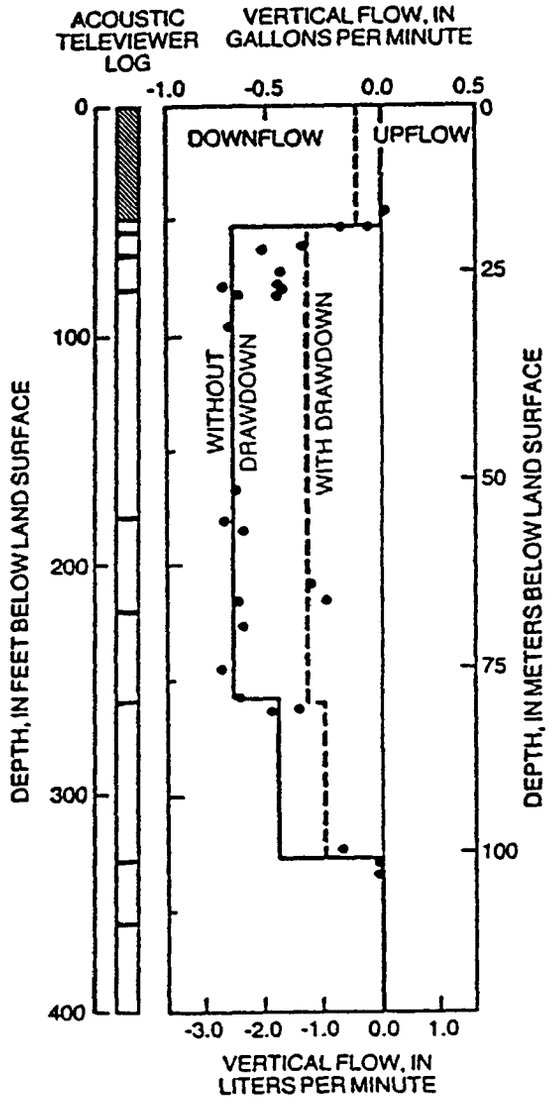

Figure III-6. Profile of Vertical Flow in a Borehole in Southeastern New York, Illustrating Downflow With and Without Drawdown in the Upper Fracture Zone.

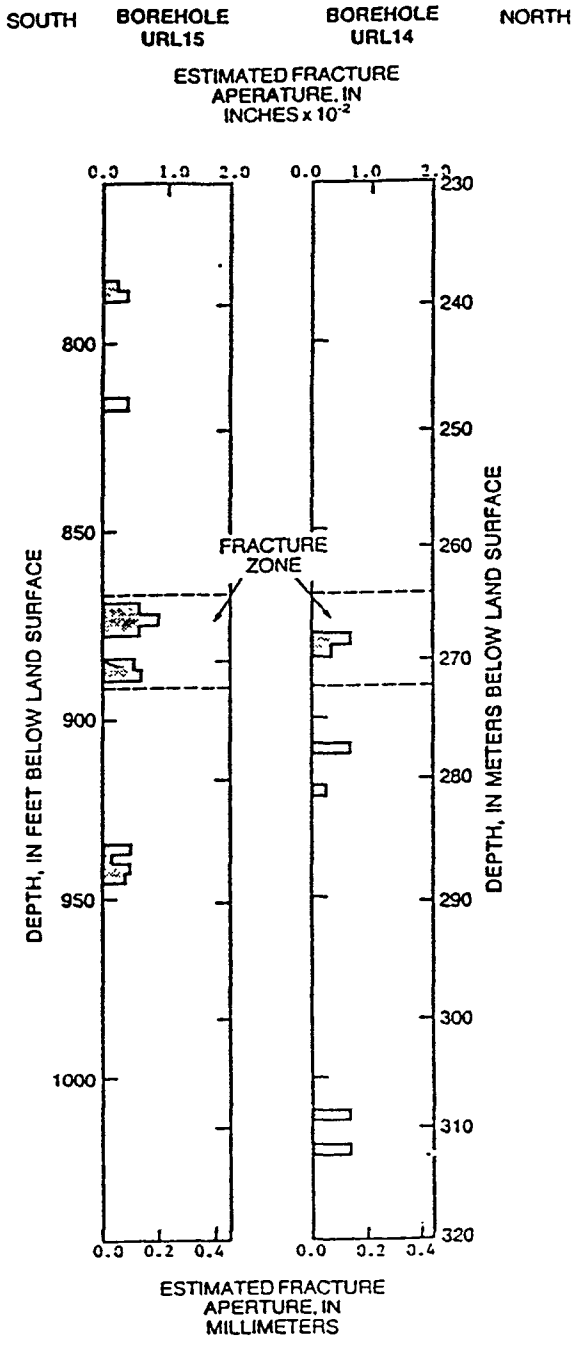

Figure III-7. Distribution of Fracture Permeability in Boreholes URL14 and URL15. Fracture Permeability is Expressed as the Aperture of a Single, Planar Fracture Capable of Transmitting an Equivalent Flow.

Flowmeter tests indicate that each borehole produced water from the vicinity of the fracture zone during pumping, but at markedly different rates. In borehole URL14, a pumping rate of only 0.07 gal/min (0.25 L/min) maintained a drawdown of more than 260 ft (80 m), while in borehole URL15 a pumping rate of 5 gal/min (19 L/min) resulted in only 5 ft (1.5 m) of drawdown. All water production in borehole URL14 came from a minor fracture, far below the major fracture zone, whereas all of the water production in borehole URL15 came from the lower one-half of the major fracture zone.

The hydraulic connection between the two boreholes was investigated by measuring flow in borehole URL15 while pumping borehole URL14. It was determined that flow entered borehole URL15 at the main fracture zone, at a depth of 880 ft (270 m), and then moved downward about 50 ft (15 m) to exit at an apparently minor fracture. Flow entered borehole URL14 at a minor fracture about 130 ft (40 m) below the main fracture zone (Figure III-8). Outflow from borehole URL15 was equal to inflow to URL14, within the measurement accuracy of the thermal flowmeter.

A projection of fracture planes indicates that there is no direct connection between the exit point in borehole URL15 and the entry point in borehole URL14. This analysis indicates that the hydraulic connection between the boreholes occurred by means of irregular fracture intersections beneath the main fracture. Although the major fracture zone was the primary producer when borehole URL15 was pumped, that zone produced no inflow in borehole URL14 when it was pumped.

Although it is difficult to understand how small fractures located away from the main fracture zone could provide the only connection between boreholes URL14 and URL15, other geophysical logs provided additional information. Local stress concentrations may have caused local rock mass dilatency accounting for this permeable pathway below the main fracture zone. This is inferred from borehole-wall breakouts, identified on acoustic-televiewer logs, and later confirmed by hydraulic fracturing stress measurements.

III-3 CONCLUSIONS

These case studies illustrate the potential application of the thermal flowmeter in investigations of slow flow in fractured aquifers. The relative ease of making thermal-flowmeter measurements permits reconnaissance of naturally occurring flows prior to hydraulic testing as well as the transient effects caused by pumping.

Thermal-flowmeter measurements interfere with attempts to control borehole conditions, as with packers, because of the flowmeter and wire line. In spite of this limitation, the simplicity and rapidity of thermal-flowmeter measurements constitute a valuable means to identify contaminant plume pathways while planning additional investigations. The thermal flowmeter is especially useful at sites where boreholes are intersected by permeable horizontal fractures or bedding planes.

Naturally occurring hydraulic head differences, between individual fracture zones, are altered greatly by the presence of open boreholes at a study site. These differences can only be studied by the expensive and time consuming use of packers to close all connections between fracture zones. The simple and direct measurement of vertical flows, caused by these head differences, can be obtained with the thermal flowmeter in a few hours. Additional improvements of the thermal-flowmeter, by adding a packer and refining techniques for flowmeter interpretation, may greatly decrease the time and effort required to characterize fractured rock aquifers using conventional hydraulic testing.

While the case studies described in this chapter did not all involve contaminated ground water, it is believed that the potential application to such sites is obvious. Hopefully, thermal flowmeters and other sensitive devices, such as the electromagnetic flowmeter being developed by the Tennessee Valley Authority, will be available commercially in the near future.

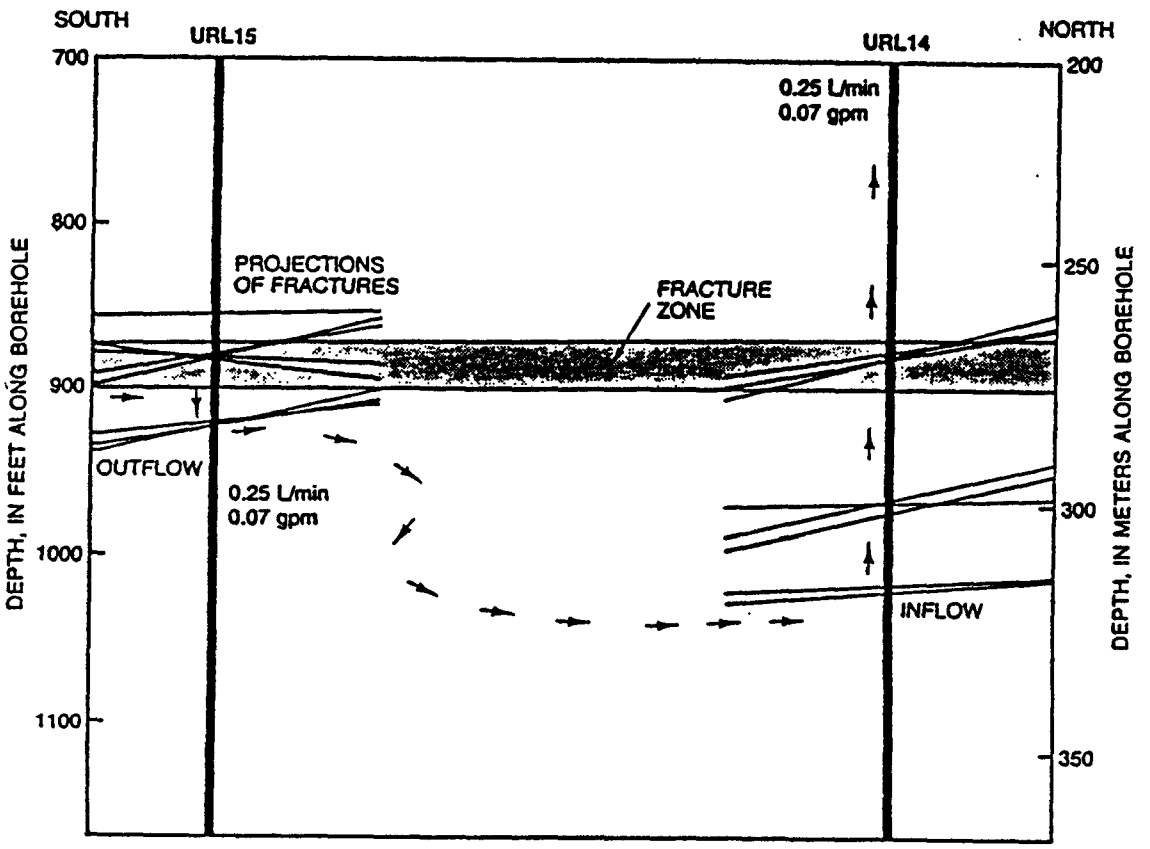

Figure III-8. Distribution of Vertical Flow Measured in Boreholes URL14 and URL15 Superimposed on the Projection of Fracture Planes Identified Using the Acoustic Televiewer.

APPENDIX I

OVERVIEW AND EVALUATION OF METHODS FOR DETERMINING THE DISTRIBUTION OF HORIZONTAL HYDRAULIC CONDUCTIVITY IN THE VERTICAL DIMENSION

AI-1 INTRODUCTION

This appendix overviews several techniques for measuring K(z), the vertical distribution of horizontal hydraulic conductivity. It is based largely on a paper by Taylor et al. (1989) published in Ground Water and should be consulted for a more in-depth evaluation of those techniques not emphasized in this report.

As discussed in the Executive Summary the application of advection-based models requires the measurement of hydraulic conductivity distributions. This has been done previously using forced gradient tracer techniques (Molz et al., 1988, 1989b), but the technology is expensive, time consuming, and usually not practical. Therefore, tracer methodology will not be discussed further here.

An important consideration when making measurements of hydraulic conductivity is the volume over which the measurement is averaged. This volume may range from a few tenths of a liter, for core studies, to hundreds or thousands of cubic meters using hydraulic testing procedures. The volume over which the measurement is made depends on the intended use of the hydraulic conductivity data. When the volume is large, important small scale features may be ignored, and when the volume is small, there may be a tendency to undersample, which can result in the loss of significant features. The exact definition of large or small depends on the local variability of hydraulic properties and the intended application of the data.

Another important consideration, with respect to hydraulic conductivity, is the significant horizontal to vertical ratio that exists in most natural formations, where anisotropy ratios on the order of 10:1 or more are common [Freeze and Cherry, 1979]. In such situations, measurements of hydraulic conductivity made in one direction are of limited value when modeling fluid movement in another. When hydraulic conductivity is treated as a scalar or a diagonalized matrix, which is usually the case, it is important that the fluid movement being modeled is consistent with the direction in which the conductivity is determined.

All borehole methods measure properties of the formation immediately surrounding the well, and the distance into the formation for which the measurement is valid is referred to as the radius of investigation. Depending on the method, the radius of investigation can range from about 0.05 to 5 m and it is important to ensure that this zone is not disturbed significantly during drilling. Morin et al. (1988b) discuss the effects of various drilling methods on the development of the disturbed zone.

AI-2 Straddle Packer Tests

One of the most common methods of determining the vertical distribution of horizontal conductivities is to perform hydraulic testing over short intervals of a borehole using a straddle packer (Fig. AI-1).

There are several variations of straddle packer tests. For example, it is common to pump into or out of a packer section at a constant rate while measuring head, or inject at a constant head while measuring flow. Another method, called the multilevel slug test, is to change the head suddenly by adding or displacing a volume of water, then recording head vs. time as the system returns to equilibrium.

In any case, these methods are accurate only if the packer is effective in hydraulically isolating a segment of the borehole. If channels exist around the well screen, fluid will bypass the packer instead of flowing radially into or out of the well as planned. Channels may be present in the structure of a well screen or caused by the failure of the formation or backfill material to fill the annulus between the casing and the borehole wall. A similar problem may occur if a gravel pack has a greater hydraulic conductivity than the formation. Although expensive, the ideal well is constructed with short screened intervals that are isolated from one another by grouting.

If leakage around the packers exists, results obtained with a straddle packer test will indicate a hydraulic conductivity that is erroneously high. To detect such leakage it is necessary to monitor the head in zones above and below the packed off interval using a pressure transducer. However, if the transmissivity of these two zones is significantly larger than that of the test zone, leakage around the straddle packer will not cause a detectable change in head outside the packed off interval. To identify this problem, it is necessary to install a second set of packers (Fig. AI-1). The hydraulic head in the segments of the well that are between the two sets of packers will now be sensitive to leakage around the first set of packers.

If the hydraulic head in the segments between the two sets of packers is influenced significantly by hydraulic testing, the straddle packer is not isolating the test segment of the well and the results will not be valid. If this situation occurs, it is usually not possible to correct and the straddle packer method cannot be used. Four packers and three transducers can be a cumbersome arrangement to operate in the field. Nevertheless, based on comparisons with other test results, the straddle packer technique worked well at the Mobile site and, therefore, was selected for detailed study.

The straddle packer method can be used to measure hydraulic conductivity over well segments that range from centimeters to hundreds of meters in length. However, the data must be analyzed carefully for small test intervals because the flow can have significant vertical components (Dagan, 1978; Melville et al., 1989). The calculated hydraulic conductivity reflects that of the formation material within 25 to 35 well radii for a typical 2 in (5 cm) well (Braester and Thunvik, 1984).

AI-3 Particle Size Methods

In a formation consisting of unconsolidated particles, the hydraulic conductivity is controlled, in part, by the size and distribution of the pores. In an effort to quantify this, Fair and Hatch (1933) and Masch and Denny (1966) have developed analytical approaches to estimate hydraulic conductivity from a description of the formation grains. The model proposed by Fair and Hatch requires that the distribution of grain sizes be known while that of Masch and Denny requires the mean and standard deviation of the grain sizes.

Both of these methods suffer from several of the fundamental problems listed below.

1. Samples must be collected during drilling. This is not always done, hence for many if not most existing wells, these methods cannot be used.

2. To determine grain-size statistics the formation must be sieved. Obviously, features such as small scale layering, compaction, and sorting are destroyed by this process. If these features exist, which is usually the case, the material to be evaluated will not be representative of the formation.

3. Bias may be introduced by the sampling method. The method may be unable to collect large material, such as gravel, or fine particles such as silt and clay.

4. The methods are limited to clean formations with sand size particles greater than 0.06 mm. Formations that have silt or clay-size material cannot be accurately analyzed with these methods.

Because of these problems, grain size analyses are limited and are unlikely to be suitable in characterizing aquifers for use in contaminant transport modeling.

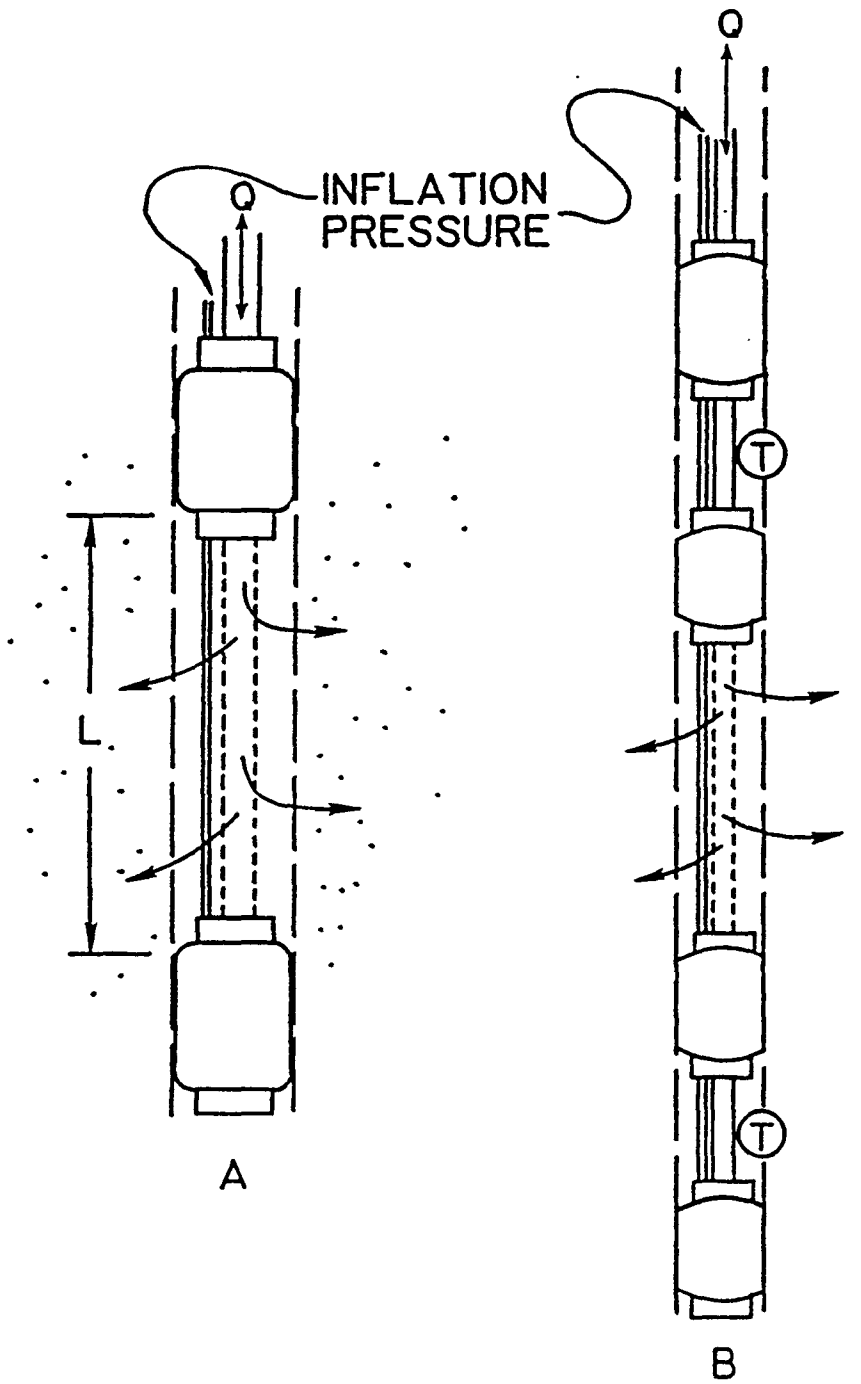

Figure AI-1. Details of an Inflatable Straddle Packer Design.

AI-4 Empirical Relationships Between Electrical and Hydraulic Conductivity

The electrical conductivity of a porous medium is a measure of its ability to conduct electrical current. In natural formations, electrical conduction occurs along two paths. The first is by ionic conduction, which is controlled by the electrical conductivity and volume of the pore fluid and the manner in which the pores are connected. The size of individual pores does not influence the electrical conductivity of the fluid. The second is along the surface of the formation matrix which is a function of the type and distribution of the matrix mineralogy, particularly with respect to the clay minerals. In clay free formations, with a constant pore fluid electrical conductivity, the electrical conductivity is usually a function of porosity. Archie's rule is a frequently used relationship relating electrical conductivity and porosity in clay-free formations (Keller and Frischknecht, 1966).

The hydraulic conductivity of a porous medium is a function of the size of the pores and the manner in which they are connected. Two formations with the same porosity, but different pores sizes, will have the same electrical conductivity but different hydraulic conductivity, so there is no clear relationship between electrical and hydraulic properties. This is further complicated when anisotropic effects are considered because the axis of anisotropy for electrical and hydraulic conductivity may not coincide. The presence of clays will further complicate any relationship between electrical and hydraulic conductivity.

Despite these problems, there are many examples in the literature of empirical relationships between electrical and hydraulic properties (Mazac et al., 1985; Kwader, 1985; Huntley, 1986; Urish, 1981). These were developed in clay free formations where electrical conduction by the matrix was not a significant factor. It is also necessary for the formation to have a relationship between porosity and hydraulic conductivity and to have a pore fluid of constant and known electrical conductivity. Depending on the formation and the methods used to measure the properties, both positive and negative correlations between the two properties have been observed. These empirical relationships are only applicable over limited areas of a specific formation. Such restrictions, and the need to measure the hydraulic conductivities at numerous locations to define the relationship, severely limit the utility of this approach. However, if a relationship can be defined, electrical measurements can be made rapidly and a large number of hydraulic conductivity determinations can be made with little additional effort.

The radius of investigation of this method is dependent on the process used to determine electrical and hydraulic conductivities. Hydraulic conductivities are usually determined by hydraulic testing and have a radius of investigation of several meters. The radius of investigation of the electrical measurements is controlled by the instrumentation and should be comparable to that of hydraulic measurements.

AI-5 Measurements Based on Natural Flow Through a Well

There are several techniques for determining the hydraulic conductivity distribution surrounding a well by measuring the natural fluid velocity distribution through the well. These are illustrated in Figure AI-2 and are most effective when the fluid velocity is horizontal. They differ according to how the velocity measurement is made within the packed off section of the well. These include heat-pulse devices for making the measurement (Melville et al., 1985) as well as various types of point-dilution approaches (Drost et al., 1968; McLinn and Palmer, 1989; Taylor et al., 1989).

In the latter approach, a tracer is injected into the segment of the well of interest where it must be kept well mixed. The tracer is removed from the segment by diffusion and advection of the fluid moving through the well. This movement is horizontal as vertical fluid movement is blocked by packers. If the velocity is high, the tracer concentration, which must be recorded, will decrease more rapidly than if the velocity is low. Since the decay is exponential, the slope of the tracer decay curve on a semi-log plot is a function of the horizontal fluid velocity.

A new type of point-dilution apparatus, based on an arrangement of dialysis cells, is illustrated in Figure AI-3. Glass cylinders having selected types of semipermeable membranes as their ends are mounted along a positioning rod. Each cell, which has a flexible rubber seal above and below, is filled with water depleted of the isotope oxygen-18, i.e. the O_{18}/O_{16} ratio is different for the water within the cell compared to the natural groundwater (Alternatively, other tracers may be used.). The entire apparatus, which may contain 20 or more

dialysis cells spaced at equal intervals along the rod, is lowered into the well and positioned within the screen. After positioning, oxygen-18 begins to diffuse into each cell with the rate of diffusion depending on the flow velocity in the vicinity of the cell. By measuring O_{18}/O_{16} ratios in each cell before and after a test, the ground water flow velocity can be calculated for each cell position. The calculation procedure is only moderately involved as described in Ronen et al., 1986, where the technique was developed and applied in an unconfined aquifer. The method was also applied at the Mobile site with some success. Once the cells and cell holders are available in large quantities, many measurements can be made rather easily.

As the title of this section implies, natural flow methods result in a velocity measurement not a hydraulic conductivity measurement. If one assumes that the head gradient is predominantly in the horizontal direction, constant with depth and with a constant porosity, K(z) will be proportional to the fluid velocity distribution v(z). An approach that results in a more direct calculation of K is described by Taylor et al., 1989.

All of the natural flow methods are relatively difficult to apply and the resulting data difficult to interpret. Due to a variety of factors, a complex flow pattern develops around a well screen that is sensitive to near-hole disturbances. Some methods require that the packed-off section be filled with glass beads, and it is difficult or impossible to achieve the same bead packing in all the measurement sections.

AI-6 Single Well Electrical Tracer (SWET) Test

In the single well electrical tracer (SWET) method (Taylor et al., 1988), salt water is injected under steady state conditions into a well. While injection of the tracer continues, the radius of invasion of the tracer is determined with a borehole induction tool (Figure AI-4). By repeatedly measuring the depth of invasion at different times, the rate of invasion can be determined. The hydraulic head, which is a measure of the driving force required to inject the fluid, is also noted. The tracer will invade different intervals of the formation at different rates depending on the hydraulic properties of each interval.

Since multiple induction logs are run, the rate of invasion can be determined at several different radii which can be converted into a hydraulic conductivity log. A porosity log can also be calculated using a model of formation electrical conductivity which accounts for variations in matrix conductivity and porosity. The SWET test procedure was field-tested for the first time at the Mobile site during the summer of 1987.

As a SWET test continues, the hydraulic conductivities calculated are representative of the formation over an increasing radius up to the radius of sensitivity of the induction tool. At the Mobile site this was on the order of 4 m, which is a relatively deep radius of investigation.

Since most wells have a disturbed zone around them, techniques having a shallow radius of investigation will be inaccurate, but the SWET test minimizes these problems. Another advantage of the SWET test is that the entire well is subjected to the same hydraulic head as opposed to the straddle packer where only a portion of the well is pressurized and errors can result if there is leakage around the packer.

A disadvantage of the SWET test is that the method requires the careful injection of a large volume of electrolyte which may not be allowed at some locations.

AI-7 Borehole Flowmeter Tests

The borehole flowmeter test is illustrated in Figure AI-5. A small pump is placed in a well and operated at a constant flow rate, Q. After near steady-state behavior is obtained the flowmeter, which measures vertical flow, is placed near the bottom of the well and a reading taken. The meter is then raised a few feet where another reading is taken. This procedure continues until the meter is above the top of the screen where the reading should equal Q, the steady state pumping rate as measured independently at the surface. As illustrated in the lower portion of Figure AI-5, the result is a series of data points giving vertical discharge within the well screen as a function of depth.

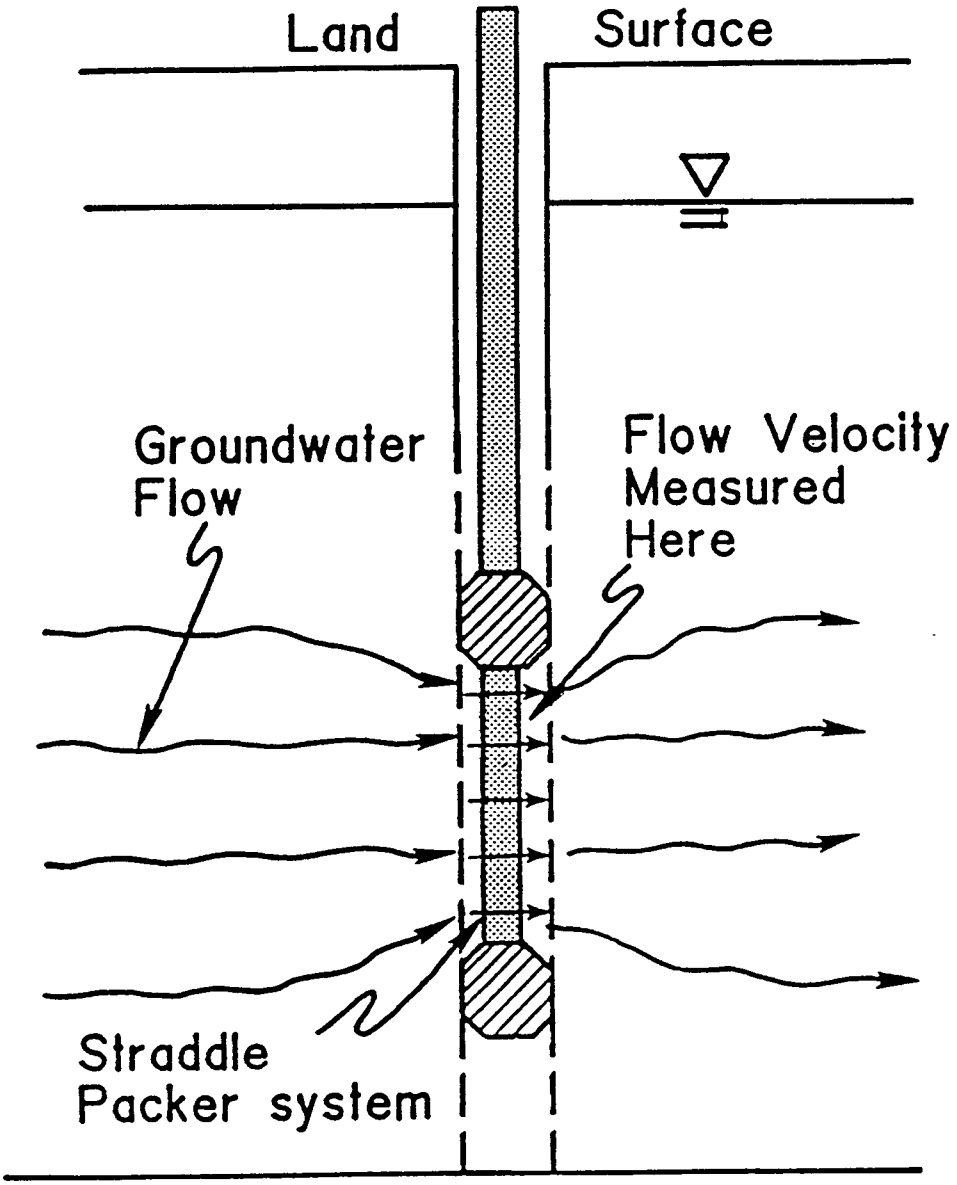

AI-2. Schematic Diagram Illustrating a Natural Flow Field in the Vicinity of a Well.

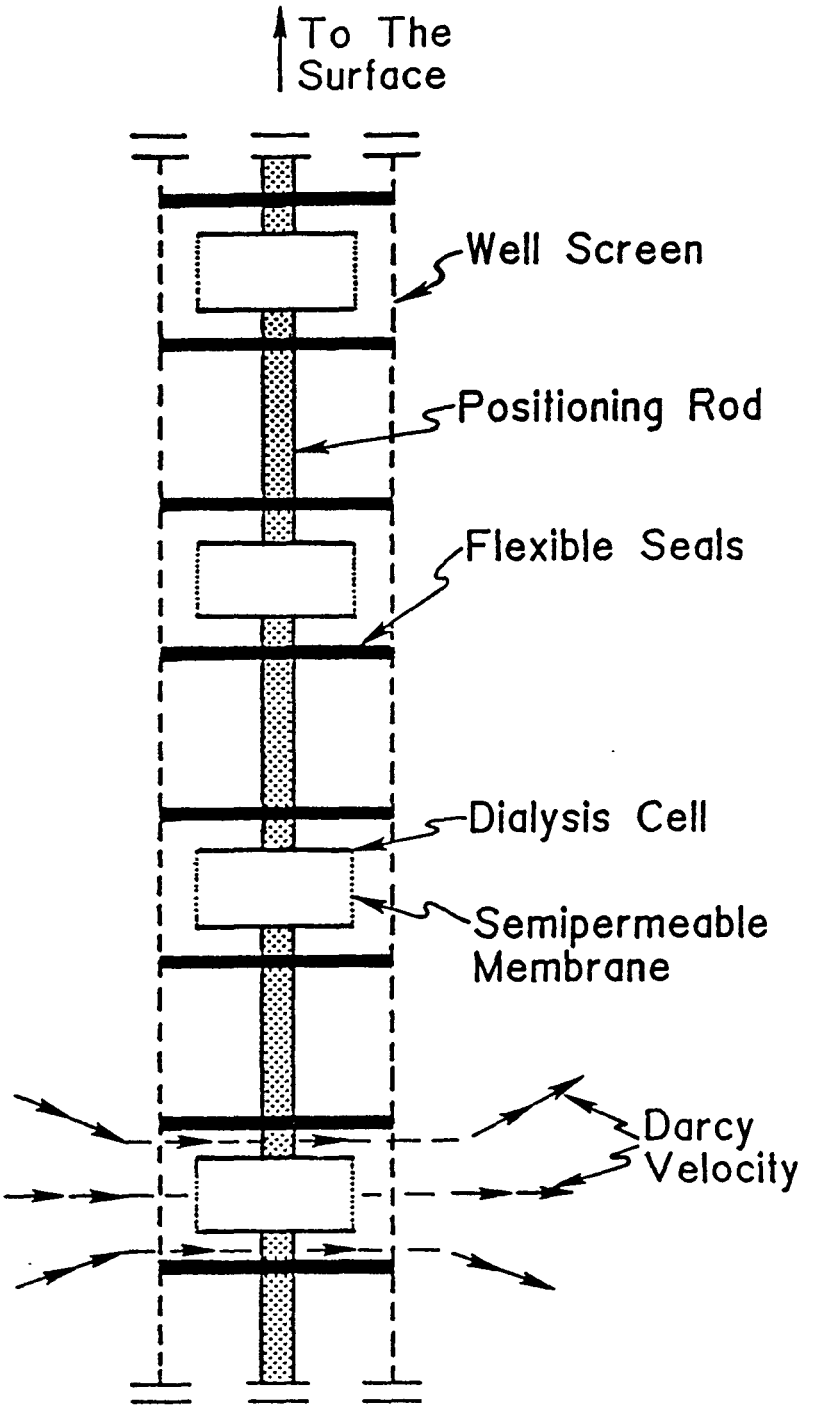

Figure AI-3. Geometry and Instrumentation Associated with the Dialysis Cell Method for Measurement of Darcy Velocity.

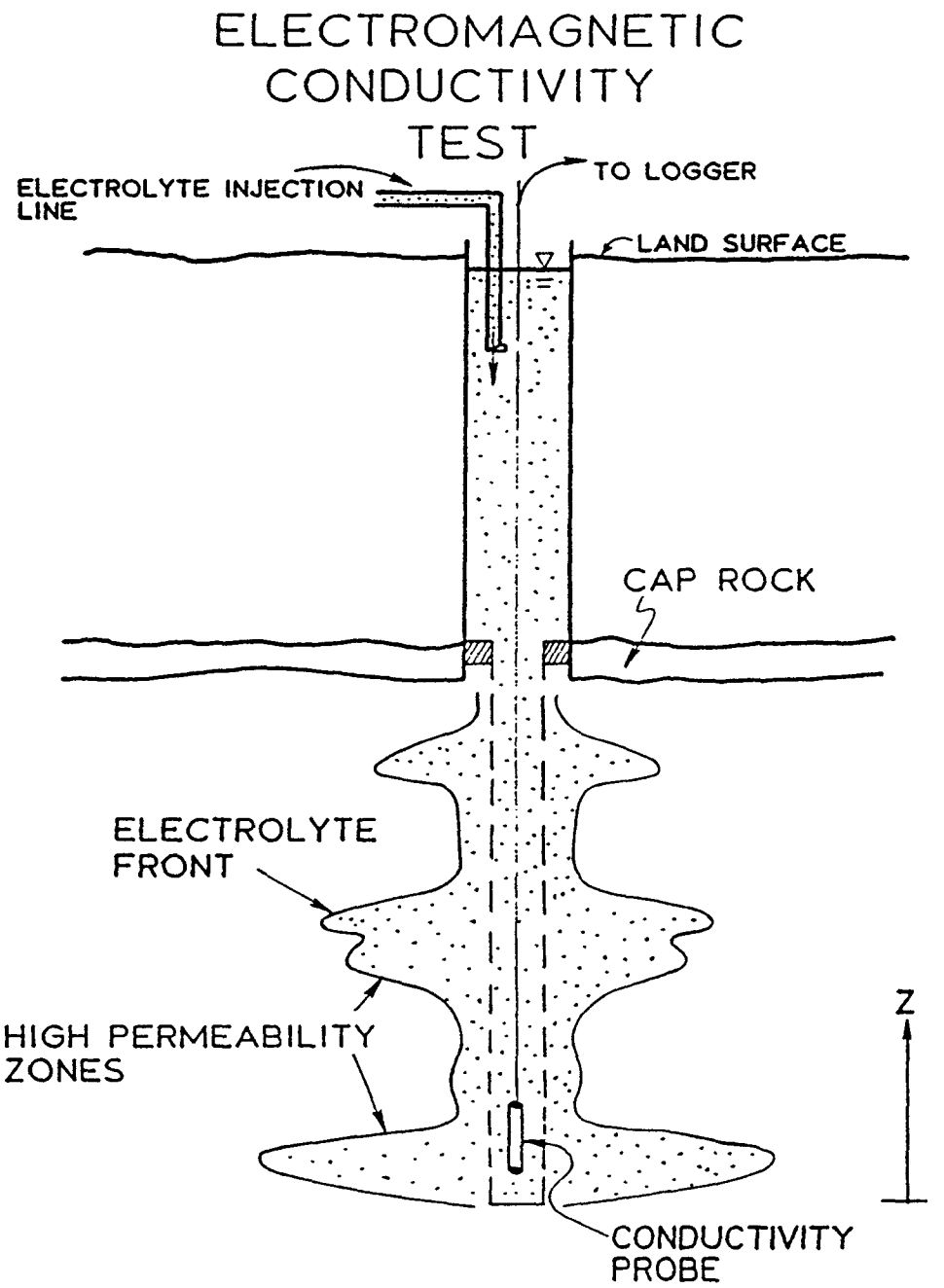

Figure AI-4. Apparatus and Geometry Associated with the SWET Test.

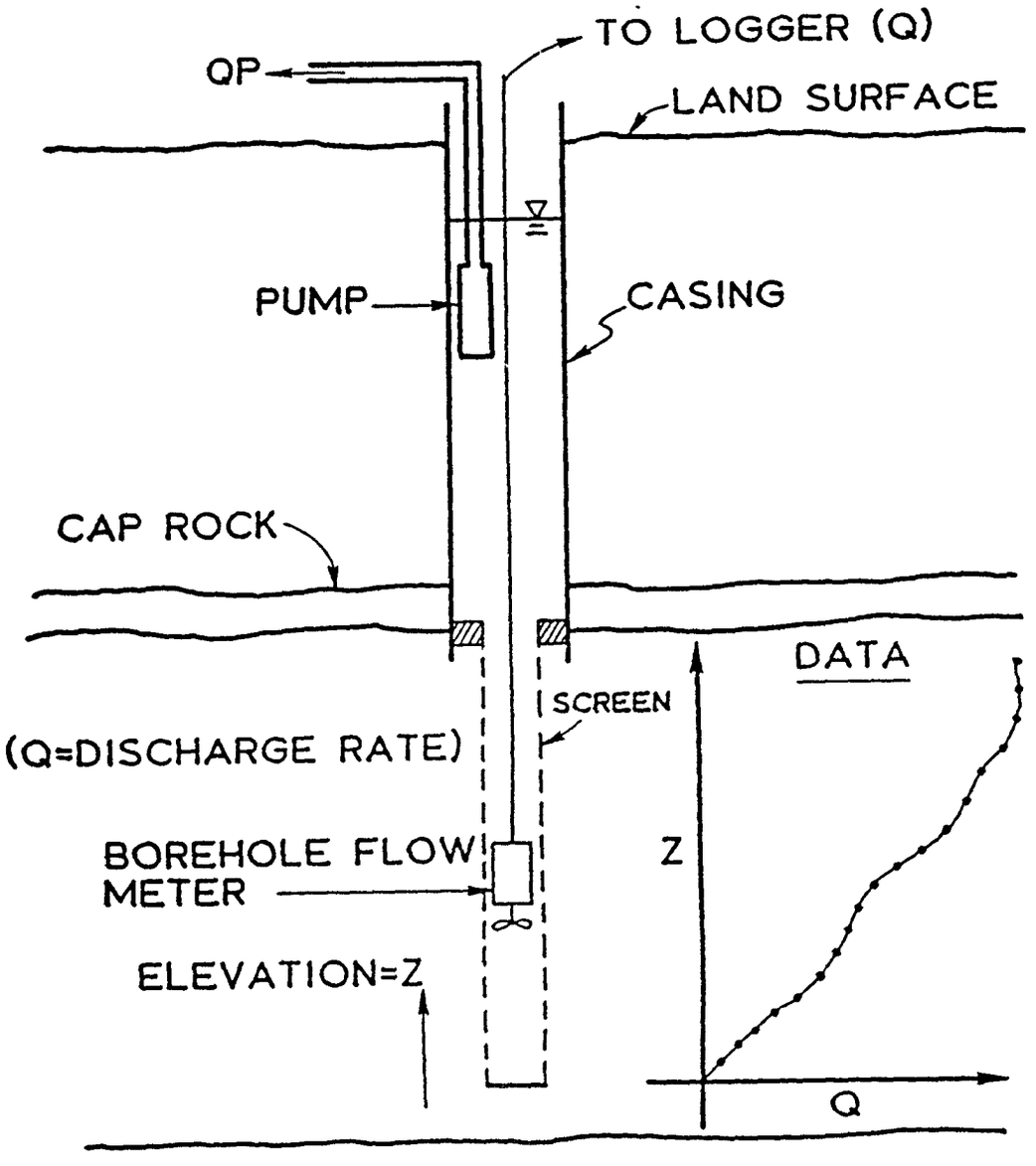

Figure AI-5. Apparatus and Geometry Associated with a Borehole Flowmeter Test.

The data analysis procedure is rather simple. The difference between two successive meter readings yields the net flow entering the screen segment between the elevations where the readings were taken. This information may be analyzed in several ways to obtain a K(z) value.

The flowmeter test suffers from the lack of readily available impeller meters designed for water well applications. Also, other types of promising technologies for flowmeter applications, such as heat-pulse (Hess and Paillet, 1989) and electromagnetic (Young and Waldrop, 1989) techniques, are not fully developed. However, it does appear that some types of heat-pulse (Hess and Paillet, 1989) and electromagnetic (Young and Waldrop, 1989) water well flow meters will be available in the near future.

AI-8 The Role of Geophysical Logging

The more traditional geophysical logging methods such as gamma logs, electric logs of various types, nuclear logs, etc., can be used to help identify the overall stratigraphy and geological setting of a site. They can also provide information of a general nature concerning hydraulic conductivity distributions. Applicable techniques are reviewed by Taylor (1989), while detailed descriptions of methods may be found in Keys and MacCary (1971), and a bibliography of borehole geophysics as applied to ground-water hydrology has been developed by Taylor and Dey (1985).

REFERENCES

Bear, J. 1979. Hydraulics of Groundwater. McGraw-Hill, New York.

Boast, C.W., and D. Kirkham. 1971. Auger hole seepage theory. Soil Science Society of America Journal, 35: 365-374.

Bouwer, H. and R.C. Rice. 1976. A slug test for determining hydraulic conductivity of unconfined aquifers with completely or partially penetrating wells. Water Resources Research, 12:423-428.

Braester, C., and R. Thunvik. 1984. Determination of formation permeability by double-packer tests. Journal of Hydrology, 72:375-389.

Bredehoeft, J.D., and S.S. Papadopulos. 1980. A method for determining the hydraulic properties of tight formations. Water Resources Research, 16:233-238.

Chapman, H.T., and A.E. Robinson. 1962. A thermal flowmeter for measuring velocity of flow in a well. U.S. Geological Survey Water-Supply Paper, 1544-E, 12.

Cooper, H.H., J.D. Bredehoeft, and S.S. Papadopulos. 1967. Response of a finite diameter well to an instantaneous charge of water. Water Resources Research, 3:263-269.

Cooper, H.H., and C.E. Jacob. 1946. A generalized graphical method for evaluating formation constants and summarizing well-field history. Transactions American Geophysical Union, 27:526-534.

Dagan, G. 1978. A note on packer, slug, and recovery tests in unconfined aquifers. Water Resources Research, 14:929-934.

Davis, S.N., G.M. Thompson, H.W. Bentley, and G. Stiles. 1980. Groundwater tracers - a short review. Ground Water, 18:14-23.

Drost, W., D. Klotz, A. Koch, H. Moser, F. Neumaier, and W. Rauert. 1968. Point dilution methods of investigating groundwater flow by means of radioisotopes. Water Resources Research, 4:125-146.

Dudgeon, C.R., M.J. Green, and W.J. Smedmore. 1975. Heat-pulse flowmeter for boreholes: Medmenham, Marlow, Bucks, England. Water Research Centre Technical Report TR-4, 69.

Fair, G.M., and L.P. Hatch. 1933. Fundamental factor governing the stream line flow of water through sands. Journal American Water Works Association, 25:1551-1565.

Freeze, R.A., and J.A. Cherry. 1979. Groundwater. Prentice-Hall, Englewood Cliffs, New Jersey, 604.

Hada, S. 1977. Utilization and interpretation of micro flowmeter. Engineering Geology (Japan), 18:26-37.

Hess, A.E. 1982. A heat-pulse flowmeter for measuring low velocities in boreholes. U.S. Geological Survey Open File Report 82-699:40 pp.

Hess, A.E. 1986. Identifying hydraulically conductive fractures with a slow-velocity borehole flowmeter. Canadian Geotechnical Journal, 23:69-78.

Hess, A.E. 1988. Characterizing fractured hydrology using a sensitive borehole flowmeter with a wire-line powered packer. International Conference on Fluid Flow in Fractured Rock, Proceedings, May, Atlanta, GA (in press).

Hess, A.E., and F.L. Paillet. 1989. Characterizing flow paths and permeability distribution in fractured rock aquifers using a sensitive thermal borehole flowmeter. Proceedings of the Conference on New Field Techniques for Quantifying the Physical and Chemical Properties of Heterogeneous Aquifers. Dallas, Texas.*

Hufschmied, P. 1983. Ermittlung der Durchlassigkeit von Lockergesteins- Grundwasserleitern, eine vergleichende Untersuchung verschiedener Feldmethoden. Doctoral Dissertation No. 7397, ETH Zurich, Switzerland.

Huntley, D. 1986. Relations between permeability and electrical resistivity in granular aquifers. Ground Water, 24:466-474.

Hvorslev, H.J. 1951. Time lag and soil permeability in ground-water observations. Bulletin 36, Waterways Experiment Station, Corps of Engineers, U.S. Army, Vicksburg, MS.

Javandel, I., and P.A. Witherspoon. 1969. A method of analyzing transient fluid flow in multilayered aquifers. Water Resources Research, 5:856-869.

Javandel, I., C. Doughty, and C.F. Tsang. 1984. Groundwater Transport: Handbook of Mathematical Models, American Geophysical Union, Washington, DC, 228 pp.

Keller, G.V., and F.C. Frischknecht. 1966. Electrical methods in geophysical prospecting. Pergamon Press, 519 pp.

Keys, W.S., and L.M. MacCary. 1971. Application of borehole geophysics to water resources investigations. Techniques of water-resources investigations of the United States Geological Survey, NTIS, Washington, DC, Book 2, Chapt. E1, 109-114.

Keys, W.S., and J.K. Sullivan. 1978. Role of borehole geophysics in defining the physical characteristics of the Raft River geothermal reservoir. Idaho Geophysics, 44:1116-1141.

Kwader, T. 1985. Estimating aquifer permeability from formation resistivity factors. Ground Water, 23:762-766.

Masch, F.D., and K.J. Denny. 1966. Grain size distribution and its effect on the permeability of unconsolidated sands. Water Resources Research, 2:665-677.

Mazac, O., W.E. Kelly, and I. Landa. 1985. A hydrogeological model for relations between electrical and hydraulic properties of aquifers. Journal of Hydrology, 79:1-19.

McLinn, E.L., and C.D. Palmer. 1989. Laboratory testing and comparison of specific conductance and electrical resistivity borehole dilution devices. Proceedings, Conference of New Field Techniques for Quantifying the Physical and Chemical Properties of Heterogeneous Aquifers. Dallas, Texas.

Melville, J.G., F.J. Molz, and O. Güven. 1985. Laboratory investigation and analysis of a ground-water flow meter. Ground Water, 23:486-495.

Melville, J.G., F.J. Molz, O. Güven and M.A. Widdowson. 1989. Multi-level slug tests with comparisons to tracer data. Ground Water, submitted for publication.

Molz, F.J., O. Güven, J.G. Melville, R.D. Crocker, and K.T. Matteson. 1986a. Performance, analysis, and simulation of a two-well tracer test at the Mobile site. Water Resources Research, 22:1031-1037.

Molz, F.J., O. Güven, J.G. Melville, and J.F. Keely. 1986b. Performance and analysis of aquifer tracer tests with implications for contaminant transport modeling. USEPA, R.S. Kerr Environmental Research Laboratory, Ada, OK 74820, EPA/600/2-86/062.

Molz, F.J., O. Güven, J.G. Melville, J.S. Nohrstedt, and J.K. Overholtzer. 1988. Forced gradient tracer tests and inferred hydraulic conductivity distributions at the Mobile site. Ground Water, 26:570-579.

Molz, F.J., R.H. Morin, A.E. Hess, J.G. Melville, and O. Güven. 1989a. The impeller meter for measuring aquifer permeability variations: evaluation and comparison with other tests. Water Resources Research, 25:1677-1683.

Molz, F.J., O. Güven, J.G. Melville, and C. Cardone. 1989b. Hydraulic conductivity measurement at different scales and contaminant transport modeling. In: Dynamics of Fluids in Hierarchical Porous Media, edited by J.H. Cushman. New York, Academic Press, in press.

Morin, R.H., A.E. Hess, and F.L. Paillet. 1988a. Determining the distribution of hydraulic conductivity in a fractured limestone aquifer by simultaneous injection and geophysical logging. Ground Water, 26:587-595.

Morin, R.H., D.R. LeBlanc, and W.E. Teasdale. 1988b. A statistical evaluation of formation disturbance produced by well-casing installation methods. Ground Water, 26:207-217.

Morrow, T.B., and S.J. Kline. 1971. The evaluation and use of hot-wire and hot-film anemometers in liquids. Stanford University, Department of Mechanical Engineering, Thermosciences Division, Report MD-25, 187 pp.

Paillet, F.L., W.S. Keys, and A.E. Hess. 1985. Effects of lithology on televiewer-log quality and fracture interpretation. Society of Professional Well Log Analysis Logging Symposium, 26th, Dallas, TX, Transactions, JJJ1-JJJ30.

Paillet, F.L., A.E. Hess, C.H. Cheng, and E.L. Hardin. 1987. Characterization of fracture permeability with high-resolution vertical flow measurements during borehole pumping. Ground Water, 25:28-40.

Paillet, F.L., and A.E. Hess. 1987. Geophysical well log analysis of fractured granitic rocks at Atikokan, Ontario, Canada. U.S. Geological Survey Water Resources Investigations Report 87-4154, 36 pp.

Papadopulos, S.S., J.D. Bredehoeft, and H.H. Cooper, Jr. 1973. On the analysis of "slug test" data. Water Resources Research, 9:1087-1089.

Parr, A.D., F.J. Molz, and J.G. Melville. 1983. Field determination of aquifer thermal energy storage parameters. Ground Water, 21:22-35.

Rehfeldt, K.R., P. Hufschmied, L.W. Gelhar, and M.E. Schaefer. 1989. The borehole flowmeter technique for measuring hydraulic conductivity variability. Report #EN-6511, Electric Power Research Institute, 3412 Hillview Ave., Palo Alto, CA.

Ronen, D., M. Magaritz, N. Paldor, and Y. Backmat. 1986. The behavior of groundwater in the vicinity of the watertable evidenced by specific discharge profiles. Water Resources Research, 22:1217-1224.

Schimschal, U. 1981. Flowmeter Analysis at Raft River, Idaho. Ground Water, 19:93-97.

Stallman, R.W. 1971. Aquifer-test design, observation and data analysis, Book 3, Chapter B1 of Techniques of Water-Resources Investigations of the United States Geological Survey.

Taylor, T.A., and J.A. Dey. 1985. Bibliography of borehole geophysics as applied to ground-water hydrology. Geological Survey Circular 926, #1985-576-049/20,029, U.S. Government Printing Office, Washington, DC.

Taylor, K., F.J. Molz, and J. Hayworth. 1988. A single well electrical tracer test for the determination of hydraulic conductivity and porosity as a function of depth. Proceedings of the Second National Outdoor Action Conference, Las Vegas, NV. May 23-26.

Taylor, K. 1989. Review of borehole methods for characterizing the heterogeneity of aquifer hydraulic properties. Proceedings of the Conference on New Field Techniques for Quantifying the Physical and Chemical Properties of Heterogeneous Aquifers. Dallas, Texas.*

Taylor, K., S.W. Wheatcraft, J. Hess, J.S. Hayworth, and F.J. Molz. 1989. Evaluation of methods for determining the vertical distribution of hydraulic conductivity. Ground Water, 27:88-98.

Urish, D.W. 1981. Electrical resistivity-hydraulic conductivity relationships in glacial outwash aquifers. Water Resources Research, 17:401-408.

U.S. Bureau of Reclamation. 1977. Groundwater Manual. Water resources technical publication, # 480.

Widdowson, M.A., F.J. Molz, and J.G. Melville. 1989. Development and application of a model for simulating microbial gorwth dynamics coupled to nutrient and oxygen transport in porous media. Proceedings, Solving Ground Water Problems with Models, Vol. 1, 28-51. National Water Well Assoc., Columbus, OH.

Young, S.C., and W.R. Waldrop. 1989. An electromagnetic borehole flowmeter for measuring hydraulic conductivity variability. Proceedings of the Conference on New Field Techniques for Quantifying the Physical and Chemical Properties of Heterogeneous Aquifers. Dallas, Texas.*

Zemanek, J., E.E. Glenn, L.J. Norton, and R.L. Caldwell. 1970. Formation evaluation by inspection with the borehole televiewer. Geophysics, 35:254-269.

*Proceedings available from: Water Resources Research Institute, 202 Hargis Hall, Auburn University, AL 36849

U.S. GOVERNMENT PRINTING OFFICE 1990/748-159/00438